Identification of Hepatic Metabolites of Two Highly Carcinogenic Polycyclic Aza-Aromatic Compounds, 7,9-Dimethylbenz[c]acridine and 7,10-Dimethylbenz[c]acridine

Yuerong Ye, Colin C. Duke, and Gerald M. Holder*

Department of Pharmacy, University of Sydney, NSW 2006, Australia

Received June 28, 1994[⊗]

The hepatic microsomal metabolites of the highly carcinogenic dimethylbenzacridines, 7,9-dimethylbenz[c]acridine (7,9-DMBAC), and 7,10-dimethylbenz[c]acridine (7,10-DMBAC) were obtained with preparations from 3-methylcholanthrene-pretreated rats. Metabolites were separated by reversed-phase HPLC and characterized using UV spectral data and chemical ionization–mass spectrometry after trimethylsilylation and GC. Comparisons with products formed in the presence of the epoxide hydrolase inhibitor, 1,1,1-trichloropropane 2,3-oxide and with those formed from the three synthetic alcohol derivatives of each parent compound, aided the assignment of firm or tentative structures to 16 products from 7,9-DMBAC found in 22 reversed-phase chromatographic peaks, and for 17 products of 7,10-DMBAC found in 19 chromatographic peaks. The more abundant metabolites were derived from oxidation of the methyl groups. Other metabolites were dihydrodiols, epoxides, phenols and secondary metabolites. The 9-methyl group prevented dihydrodiol formation at the 8,9-position from 7,9-DMBAC, and for each carcinogen, the 3,4-dihydrodiol was formed. As well, 3,4-dihydrodiols of methyl oxidized compounds were found.

Introduction

Polycyclic aza-aromatic hydrocarbons (PAAH)[1] are among the nitrogen-containing environmental contaminants that humans are exposed to, inhale, or ingest. Other groups of tumorigenic substances are the nitroaromatic compounds, heterocyclic amines found as food mutagens, aromatic amines, and nitrosamines. For the PAAH, studies have been conducted to determine the metabolites of quinoline, isoquinoline (*1*), methylquinolines (*2*), acridine, benzo[*f*]quinoline, benzo[*h*]quinoline, benz[*a*]acridine, benz[*c*]acridine, 7-methylbenz[*c*]acridine (7MBAC), dibenzo[*c*,*h*]carbazole, and dibenz[*a*,*j*]acridine. Studies on systems of three rings or greater and the biological properties of these compounds have been recently reviewed (*3*). Compared with the non-nitrogenous compound, benz[*a*]anthracene, benz[*c*]acridine is a more potent carcinogen. Its methylated derivative, 7MBAC, has even greater activity (*4*). The tumorigenic activities of the 7,9-dimethylbenz[*c*]acridine (7,9-DMBAC), 7,10-dimethylbenz[*c*]acridine (7,10-DMBAC) (Figure 1), and 7,9,10-trimethylbenz[*c*]acridine in mouse painting tests without promotion were equal to or greater than that of 7MBAC. The dimethyl derivatives were also active after subcutaneous injection leading to local sarcomas (*5*). Compounds with longer alkyl groups at the 7-position in the 7,9-substituted series displayed reduced activity, but 9-fluoro-7-methylbenz[*c*]acridine was highly active. In contrast, the benz[*a*]acridines were inactive or only weakly active. Although 7,12-dimethylbenz[*a*]anthracene has been extensively studied (*6, 7*), no metabolic work has been carried out on these potent dialkylbenz[*c*]acridines. These compounds have potential environmental significance because such substances have been reported to be present in the atmosphere (*8, 9*).

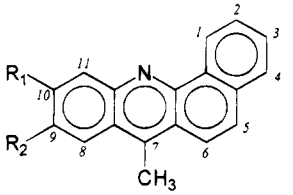

7,9-DMBAC: R_1 = H; R_2 = CH_3

7,10-DMBAC: R_1 = CH_3; R_2 = H

Figure 1. Structures of 7,9-dimethylbenz[*c*]acridine (7,9-DMBAC) and 7,10-dimethylbenz[*c*]acridine (7,10-DMBAC).

In the detailed metabolic studies of the polycyclic aromatic hydrocarbon (PAH) 7,12-dimethylbenz[*a*]anthracene, several products were characterized (*6, 7*). Other alkyl PAH (*7*) and PAAH (*3, 10*) have also been investigated, and in all these studies liver microsomal catalyzed oxidation of the methyl group has been a predominant pathway. The present study was undertaken to identify the *in vitro* hepatic metabolic products formed from two potent benz[*c*]acridines, 7,9-DMBAC and 7,10-DMBAC, with the intention of characterizing those metabolites associated with their activation pathways. Minor metabolites were investigated because active metabolites are often of less importance quantitatively (*7, 11, 12*), and because secondary metabolites,

* To whom correspondence should be addressed.

[⊗] Abstract published in *Advance ACS Abstracts,* January 15, 1995.

[1] Abbreviations: PAAH, polycyclic aza-aromatic hydrocarbons; 7MBAC, 7-methylbenz[*c*]acridine; 7,9-DMBAC and 7,10-DMBAC, isomeric dimethylbenz[*c*]acridines; 3MC, 3-methylcholanthrene; TCPO, 1,1,1-trichloropropane 2,3-oxide; G-6-P, glucose 6-phosphate; G-6-PDH, glucose-6-phosphate dehydrogenase; CIMS, chemical ionization mass spectrometry; GCMS, gas chromatography/mass spectrometry; 7-OHM-9MBAC, 7-(hydroxymethyl)-9-methylbenz[*c*]acridine; 9-OHM-7MBAC, 9-(hydroxymethyl)-7-methylbenz[*c*]acridine; 7,9-diOHMBAC, 7,9-bis-(hydroxymethyl)benz[*c*]acridine; 7-OHM-10MBAC, 7-(hydroxymethyl)-10-methylbenz[*c*]acridine; 10-OHM-7MBAC, 10-(hydroxymethyl)-7-methylbenz[*c*]acridine; 7,10-diOHMBAC, 7,10-bis(hydroxymethyl)-benz[*c*]acridine; 7,9-DMBAC-5,6-oxide, 7,9-dimethylbenz[*c*]acridine 5,6-oxide; 7,12-DMBA, 7,12-dimethylbenz[*a*]anthracene.

0893-228x/95/2708-0188$09.00/0

generally formed in lesser abundance, have also been associated with bioactivations (*13, 14*).

Experimental Procedures

Caution. *All compounds in this study are potential carcinogenic agents and should be handled in an appropriate manner.*

Chemicals. 3-Methylcholanthrene (3MC) was obtained from Sigma Chemical Co. (St. Louis, MO). Bovine serum albumin, glucose 6-phosphate (G-6-P), glucose-6-phosphate dehydrogenase (G-6-PDH), and NADP were purchased from Boehringer Mannheim (Sydney, Australia). 1,1,1-Trichloropropane 2,3-oxide (TCPO) was obtained from Aldrich Chemical Co. Inc. (Milwaukee, WI). Tri-Sil (1% hexamethyldisilazane and 1% trimethylsilyl chloride in pyridine) was from Pierce Chemical Co. (Rockford, IL). 7,9-DMBAC (*14*), 7,10-DMBAC (*15*), and bromomethyl derivatives of both compounds (*16*) were prepared by literature methods. Preparative short column vacuum chromatography (*17*) was effected using silica gel (Keiselgel H, E Merck, Darmstadt, Germany). Generally, melting points were determined for new compounds, and characterization was by ^{1}H NMR and high resolution electron impact spectrometry of chromatographically pure material.

Instrumentation. ^{1}H NMR spectra were obtained in $CDCl_3$ unless otherwise noted using a JEOL FX90Q (89.6 MHz), Bruker W.M. (400 MHz), or a Varian Gemini (300 MHz) spectrometer. Chemical ionization mass spectra (CIMS) were obtained using methane as reagent gas with a Finnigan TSQ46 triple-stage quadrupole instrument and the solid probe or GC interface. High resolution electron impact spectra were determined with an AEI MS902. Composition matches were considered acceptable when they lay within 10 ppm of calculated values since the hazardous nature of these compounds required introduction of the materials into the spectrometer in glass mp tubes, and the number of individual determinations was limited. The usual deviation allowed is 5 ppm. All compounds were chromatographically pure. HPLC were generally run on a dual 126 pump Beckman system configuration which included a 168 linear diode array spectrophotometric detector. This allowed spectra of metabolites emerging from the chromatographic column to be obtained.

7,10-Dimethylbenz[c]acridine (7,10-DMBAC). The product obtained by the Bernthsen reaction (*14, 18*) from *N-m*-tolyl-1-naphthylamine (*19*) was chromatographed to yield a mixture of 7,10-DMBAC and 7,8-dimethylbenz[c]acridine (85:15 by HPLC, GC, and ^{1}H NMR by integration of the 10-methyl and 8-methyl signals at δ 2.76 and 2.93 ppm, respectively). Further chromatography gave a fraction with only 6% of the 7,8-isomer, and fractional crystallization afforded >98% pure 7,10-DMBAC: mp 155–156 °C [lit. mp 152 °C (*15*)]; ^{1}H NMR δ (ppm) 9.54 (bd, H_1), 7.36–8.17 (m, 8 aromatic protons), 3.09 (s, 7-CH_3), 2.63 (s, 10-CH_3); CIMS *m/z* (rel intensity) 258 (MH^+, 100), 286 ($M + C_2H_5^+$, 22), 298 ($M + C_3H_5^+$, 6).

7-(Hydroxymethyl)-9-methylbenz[c]acridine (7-OHM-9MBAC). 7-(Bromomethyl)-9-methylbenz[c]acridine (*16*) (4 mg) was heated under reflux with potassium acetate (4 mg) in ethanol (2 mL) under N_2 for 2 h. Removal of the solvent, extraction of the products in EtOAc solution with 5% $NaHCO_3$, and vacuum chromatography on silica afforded 7-(acetoxymethyl)-9-methylbenz[c]acridine (2.5 mg, 63%), mp 160–162 °C, as a yellow solid: ^{1}H NMR δ (ppm) 9.51 (m, H_1), 8.30[2] (d, $J_{10,11}$ = 8.8 Hz, H_{11}), 8.09 (d, $J_{5,6}$ = 9.5 Hz, H_6), 8.07 (bs, H_8), 7.62–7.94 (m, 5 aromatic protons), 6.08 (s, 7-methylene), 2.65 (s, 9-CH_3), 2.12 (s, acetate CH_3); CIMS *m/z* (rel intensity) 316 (MH^+, 100), 344 ($M + C_2H_5^+$, 18), 356 ($M + C_3H_5^+$, 5), 256 ($MH^+ - CH_3COOH$, 75); high resolution electron impact MS *m/z* 315.1242 ($C_{21}H_{17}NO_2$ requires 315.1259).

Treatment of the acetate with 0.05 M NaOH in 95% ethanol (2 mL) at room temperature for 0.5 h was followed by removal of the solvent and isolation of the products by extraction of an EtOAc solution with water and brine. Vacuum chromatography on silica afforded 7-OHM-9MBAC (2 mg): mp 164–167 °C; ^{1}H NMR δ (ppm) 9.43 (m, H_1), 8.19 (d, $J_{10,11}$ = 8.1 Hz, H_{11}), 8.02 (d, $J_{5,6}$ = 9.0 Hz, H_6), 8.00 (bs, H_8), 7.51–7.90 (m, 5 aromatic protons), 5.53 (d, 7-methylene), 2.82 (bs, OH, exchangeable with D_2O), 2.54 (s, 9-CH_3); CIMS *m/z* (rel intensity) 274 (MH^+, 100), 302 ($M + C_2H_5^+$, 15), 314 ($M + C_3H_5^+$, 4), 256 ($MH^+ - H_2O$, 62), 244 (6); high resolution electron impact MS *m/z* 273.1149 ($C_{19}H_{15}NO$ requires 273.1153).

9-(Hydroxymethyl)-7-methylbenz[c]acridine (9-OHM-7MBAC). This was prepared from 9-(bromomethyl)-7-methylbenz[c]acridine (*16*) via the acetoxymethyl compound as above for 7-OHM-9MBAC. 9-(Acetoxymethyl)-7-methylbenz[c]acridine possessed mp 130–133 °C; ^{1}H NMR δ (ppm) 9.53 (m, H_1), 8.34 (d, $J_{10,11}$ = 9.0 Hz, H_{11}), 8.23 (bs, H_8), 8.04 (d, $J_{5,6}$ = 9.9 Hz, H_6), 7.68–7.93 (m, 5 aromatic protons), 5.38 (s, 9-methylene), 3.10 (s, 7-CH_3), 2.18 (s, acetate CH_3); CIMS *m/z* (rel intensities) 316 (MH^+, 100), 344 ($M + C_2H_5^+$, 16), 356 ($M + C_3H_5^+$, 5), 256 ($MH^+ - CH_3COOH$, 100); high resolution electron impact MS *m/z* 315.1266 ($C_{21}H_{17}NO_2$ requires 315.1259).

9-OHM-7MBAC was a light yellow solid: mp 114.5–117.5 °C; ^{1}H NMR δ (ppm) 9.51 (m, H_1), 8.29 (d, $J_{10,11}$ = 9.0 Hz, H_{11}), 8.11 (bs, H_8), 7.99 (d, $J_{5,6}$ = 9.0 Hz, H_6), 7.64–7.87 (m, 5 aromatic protons), 4.92 (s, 9-methylene), 3.02 (s, 7-CH_3), 2.09 (bs, OH, disappears after treatment with D_2O); CIMS *m/z* (rel intensity) 274 (MH^+, 100), 302 ($M + C_2H_5^+$, 17), 314 ($M + C_3H_5^+$, 6), 256 ($MH^+ - H_2O$, 48), 244 (12); high resolution electron impact MS *m/z* 273.1136 ($C_{19}H_{15}NO$ requires 273.1153).

7,9-Bis(hydroxymethyl)benz[c]acridine (7,9-diOHM-BAC). 7,9-Bis(bromomethyl)benz[c]acridine (*16*) (8 mg) was treated with potassium acetate (6 mg) in EtOH (2.0 mL) under reflux and afforded, after workup described above, 7,9-bis-(acetoxymethyl)benz[c]acridine (4 mg, 55%): mp 152–156 °C; ^{1}H NMR δ (ppm) 9.46 (m, H_1), 8.34 (d, $J_{10,11}$ = 9.0 Hz, H_{11}), 8.24 (bs, H_8), 8.05 (d, $J_{5,6}$ = 9.5 Hz, H_6), 7.65–7.86 (m, 5 aromatic protons), 6.03 (s, 7-methylene), 5.33 (s, 9-methylene), 2.13 (s, 7-acetate methyl), 2.05 (s, 9-acetate methyl); CIMS *m/z* (rel intensity) 374 (MH^+, 38), 402 ($M + C_2H_5^+$, 11), 414 ($M + C_3H_5^+$, 3), 314 ($MH^+ - CH_3COOH$, 100), 256 (15); high resolution electron impact MS *m/z* 373.1308 ($C_{23}H_{19}NO_4$ requires 373.1314).

7,9-DiOHMBAC was isolated by hydrolysis as described above as yellow needles: mp 174–176 °C; ^{1}H NMR δ (ppm, acetone-d_6) 9.51 (H_1, m), 8.53 (bs, H_8), 8.36 (d, $J_{10,11}$ = 9.9 Hz, H_{11}), 8.31 (d, $J_{5,6}$ = 9.9 Hz, H_6), 7.72–8.08 (m, 5 aromatic protons), 5.63 (bs, 7-methylene), 4.94 (bs, 9-methylene), 3.11 and 2.09 (bs, OH protons, exchangeable with D_2O); CIMS *m/z* (rel intensity): 290 (MH^+, 90), 318 ($M + C_2H_5^+$, 16), 330 ($M + C_3H_5^+$, 4), 272 ($MH^+ - H_2O$, 100); high resolution electron impact MS *m/z* 289.1105 ($C_{19}H_{15}NO_2$ requires 289.1103).

7-(Hydroxymethyl)-10-methylbenz[c]acridine (7-OHM-10MBAC). 7-(Acetoxymethyl)-10-methylbenz[c]acridine was obtained from 7-(bromomethyl)benz[c]acridine (*16*) (5 mg) as a light yellow solid: mp 151–153 °C; ^{1}H NMR δ (ppm) 9.47 (m, H_1) 8.22 (d, $J_{8,9} \approx 9$ Hz, H_8), 8.17 (bs, H_{11}), 8.07 (d, $J_{5,6} \approx 9$ Hz, H_6), 7.41–7.85 (m, 5 aromatic protons), 6.06 (s, 7-methylene), 2.64 (s, 10-methyl), 2.09 (s, acetate methyl); CIMS *m/z* (rel intensity) 316 (MH^+, 100), 344 ($M + C_2H_5^+$, 20), 356 ($M + C_3H_5^+$, 4), 256 ($MH^+ - CH_3COOH$, 88); high resolution electron impact MS *m/z* 315.1229 ($C_{21}H_{17}NO_2$ requires 315.1259).

Hydrolysis of the acetate as described for 7-OHM-9MBAC gave 7-OHM-10MBAC: mp 148–151 °C; ^{1}H NMR δ (ppm) 9.40 (m, H_1), 7.83–8.07 (m, H_6, H_8 and H_{11}), 7.15–7.80 (m, 4 aromatic protons), 7.51 (d, J = 9.0 Hz, H_5 or H_9), 5.42 (bs, 7-methylene), 2.82 (bs, OH, exchangeable with D_2O), 2.55 (s, 10-methyl); CIMS *m/z* (rel intensity) 274 (MH^+, 100), 302 ($M + C_2H_5^+$, 20), 314 ($M + C_3H_5^+$, 6), 256 ($MH^+ - H_2O$, 69), 244 (19); high resolution electron impact MS *m/z* 273.1133 ($C_{19}H_{15}NO$ requires 273.1153).

10-(Hydroxymethyl)-7-methylbenz[c]acridine (10-OHM-7MBAC). This was prepared from 10-(bromomethyl)-7-methylbenz[c]acridine as described above for 7-OHM-9MBAC through the acetate, 10-(acetoxymethyl)-7-methylbenz[c]acridine: mp 78–82 °C; ^{1}H NMR δ (ppm) 9.53 (m, H_1), 8.34 (bs, H_{11}), 8.27 (d, $J_{8,9}$ = 9.0 Hz, H_8), 8.04 (d, $J_{5,6}$ = 9.0 Hz, H_6), 7.51–7.88 (m, 5 aromatic protons), 5.40 (s, 10-methylene), 3.10 (s, 7-methyl), 2.20 (s, acetate methyl); CIMS *m/z* (rel intensity) 316 (MH^+, 83), 344 ($M + C_2H_5^+$, 18), 356 ($M + C_3H_5^+$, 6), 256 ($MH^+ - CH_3COOH$,

[2] Here, and elsewhere below, the assignment of H_5 or H_6 and H_{11} may be reversed. In the 7,10-DMBAC series the reversal may be between H_5 or H_6 and H_8.

100); high resolution electron impact MS m/z 315.1275 ($C_{21}H_{17}NO_2$ requires 315.1259).

10-OHM-7MBAC possessed mp 146–150 °C; ^{1}H NMR δ (ppm) 9.53 (m, H_1), 8.32 (bs, H_{11}), 8.25 (d, $J_{8,9}$ = 9.0 Hz, H_8), 8.02 (d, $J_{5,6}$ = 9.0 Hz, H_6), 7.67–7.88 (m, 5 aromatic protons), 4.99 (bs, 10-methylene), 3.08 (s, 7-methyl), 2.09 (bs, OH, exchangeable with D_2O); CIMS m/z (rel intensity): 274 (MH^+, 100), 302 (M + $C_2H_5^+$, 18), 314 (M + $C_3H_5^+$, 4), 256 ($MH^+ - H_2O$, 69), 244 (19); high resolution electron impact m/z 273.1173 ($C_{19}H_{15}NO_2$ requires 273.1153).

7,10-Bis(hydroxymethyl)benz[*c*]acridine (7,10-diOHMBAC). This was prepared as described above from 7,10-bis(bromomethyl)benz[*c*]acridine (*16*) (4 mg). 7,10-Bis(acetoxymethyl)benz[*c*]acridine was a light yellow solid: mp 125–128°C; ^{1}H NMR δ (ppm) 9.51 (m, H_1), 8.37 (bs, H_{11}), 8.36 (d, $J_{8,9}$ = 8.1 Hz, H_8), 8.11 (d, $J_{5,6}$ = 9.0 Hz, H_6), 7.56–7.93 (m, 5 aromatic protons), 6.09 (s, 7-methylene), 5.41 (s, 10-methylene), 2.21 (s, 7-acetate methyl), 2.10 (s, 10-acetate methyl); CIMS m/z (rel intensity) 374 (MH^+, 47), 402 (M + $C_2H_5^+$, 8), 414 (M + $C_3H_5^+$, 3), 314 ($MH^+ - CH_3CO_2H$, 100), 256 (21); high resolution electron impact MS m/z 373.1350 ($C_{23}H_{19}NO_2$ requires 373.1314).

Hydrolysis afforded 7,10-diOHMBAC, mp 161–164 °C, as a yellow solid: ^{1}H NMR δ (ppm, acetone-d_6) 9.50 (m, H_1), 8.51 (d, $J_{8,9}$ = 9.0 Hz, H_8), 8.30 (bs, H_{11}), 8.22 (d, $J_{5,6}$ = 9.0 Hz, H_6), 7.62–8.00 (m, 5 aromatic protons), 5.63 (bs, 7-methylene), 4.96 (bs, 10-methylene), 3.11 (broad, 2 OH, exchangeable with D_2O); CIMS m/z (rel intensity) 290 (MH^+, 70), 318 (M + $C_2H_5^+$, 14), 330 (M + $C_3H_5^+$, 3), 272 ($MH^+ - H_2O$, 100); high resolution electron impact MS 289.1102 ($C_{19}H_{15}NO_2$ requires 289.1103).

7,9-Dimethylbenz[*c*]acridine 5,6-Oxide (7,9-DMBAC-5,6-oxide). 7,9-DMBAC (200 mg) in chloroform (20 mL) was vigorously stirred with 0.6 M sodium hypochlorite in 0.8 M sodium phosphate buffer (pH 8.5; 60 mL) containing tetra-*tert*-butylammonium hydrogen sulfate (136 mg) at room temperature for 1.5 h (*20*). The organic phase was washed with 0.1 M sodium phosphate (pH 8.5), dried with K_2CO_3, and evaporated to dryness. Vacuum chromatography on a short silica gel column eluted with CH_2Cl_2/petroleum spirit, bp 70–75 °C (1:1), afforded 7,9-DMBAC-5,6-oxide (50 mg, 24%), mp 157–160 °C, as a yellow solid after crystallization from CH_2Cl_2/petroleum spirit: ^{1}H NMR δ (ppm) 8.97 (m, H_1), 8.02 (m, H_{11}), 7.41–7.76 (m, 5 aromatic protons), 4.80 (d, H_6, $J_{5,6}$ = 4.1 Hz), 4.39 (dd, H_5, $J_{1,5}$ = 0.7 Hz), 2.88 (s, 7-methyl), 2.58 (s, 9-methyl); CIMS m/z (rel intensity) 274 (MH^+, 100), 302 (M + $C_2H_5^+$, 22), 314 (M + $C_3H_5^+$, 6), 258 ($MH^+ - O$, 48).

[*9-methyl*-^{3}H]7,9-DMBAC and [*10-methyl*-^{3}H]7,10-DMBAC. These were prepared and purified by reversed-phase HPLC on Lichrospher RP-8 as described (*11*). Their initial high specific radioactivities of 1.18 and 0.20 Ci/mmol were reduced by addition of unlabeled material (*14, 15*). Their radiochemical purities determined by HPLC were 99.6% and 98.9%, respectively.

Reversed-Phase HPLC. 7,9-DMBAC metabolites were separated on a Hibar 10 μm Lichrosorb-RP8 column (250 × 4.6 mm i.d.) (E Merck, Darmstadt, FRG) or a 5 μm Ultrasphere ODS column (250 × 4.6 mm i.d., Beckman Instruments, San Ramon, CA) using an acetonitrile–water gradient. This consisted of a sequence of linear increases in the proportion of organic modifier: 24–33.5% acetonitrile over 30 min, 33.5–52% acetonitrile over 20 min, 10 min isocratic elution at 52.5% acetonitrile, 52.5–76.3% acetonitrile over 10 min, and 76.3–100% acetonitrile over 1 min at a flow rate of 0.8 mL/min.

7,10-DMBAC metabolites were separated on the Hibar-RP8 column using a linear ramp gradient consisting of acetonitrile and water: 32%-40% acetonitrile over 30 min, 40–66% acetonitrile over 15 min, 20 min isocratic elution at 66%, and 66–100% acetonitrile over 10 min with a flow rate of 0.8 mL/min.

Normal-Phase HPLC. A 10 μm Lichrosorb silica column (250 × 4.6 mm i.d.) was eluted with 5% EtOH in petroleum spirit, bp 70–75 °C, at 0.8 mL/min for 7,9-DMBAC products. EtOAc (10%) in petroleum spirit, bp 70–75 °C, at 2.0 mL/min was used for 7,10-DMBAC metabolites.

The metabolite distributions and the extent of metabolism were determined by liquid scintillation radiochemical determination of fractions emerging from the reversed-phase HPLC column. The extent of metabolism was calculated from the EtOAc-soluble radioactivity which emerges from the reversed-phase column before the parent compound expressed as a fraction (%) of the total radioactivity eluted from the column.

Gas Chromatography/Mass Spectrometry (GCMS). A nonpolar HP-1 dimethylpolysiloxane coating on a silica capillary column (8.3 m × 0.2 mm i.d., Hewlett-Packard) was linked to a Finnigan-MAT triple-stage quadrupole mass spectrometer (TSQ46) or a Finnigan quadrupole 4021 operated in the chemical ionization mode with methane using helium as carrier (4 mL/min). The temperature was held at 180 °C for 2 min and then ramped to 260 °C at 15 C°/min, then raised to 300 °C at 20 C°/min, and then held constant for a further 2 min. An injection temperature of 240 °C was used, the ion source was operated at 140 °C for the TSQ46 and 220 °C for the 4021, and the electron energy was 100 eV. Mass spectral scans were taken at 120/min.

Samples were generally evaporated to dryness in Reactivials (Pierce Chemical Co.) using a stream of pure dry nitrogen, stored overnight over phosphorus pentoxide under vacuum, and derivatized at 70 °C with Tri-Sil reagent (20 μL) for 10 min to afford solutions containing 20–50 ng/μL of analyte.

Liver Fractions. Liver microsomal fractions and 9000*g* supernatants were prepared from 200 g male Sprague-Dawley rats pretreated intraperitoneally with 3MC (20 mg/kg in corn oil daily for 2 days). Animals were starved for 24 h after the last dose of inducer, killed by cervical dislocation, and then their livers were removed and washed in ice-cold 0.1 M potassium phosphate buffer (pH 7.4). They were cut with scissors, homogenized in 3 volumes of ice-cold buffer using a Waring blender (30 s), and centrifuged at 9000*g* for 30 min to afford the 9000*g* supernatant. These supernatants were then centrifuged at 100000*g* for 1 h to afford the microsomal pellets which were washed by resuspension in phosphate buffer with a Potter–Elvehjem homogenizer. After recentrifugation at 100000*g* for 30 min the microsomal pellets were resuspended with a Potter–Elvehjem homogenizer in phosphate buffer (pH 7.4) containing 20% w/v glycerol at 1 mL/g liver and stored in 1–3 mL volumes at −80 °C before use. Protein was determined using bovine serum albumin as standard (*21*), and cytochrome P450 was measured by the reduced carbon monoxide difference spectrum (*22*). Microsomes from livers of 3MC-induced rats contained 1.38 ● 0.02 (n = 3) nmol of cytochrome P450/mg of protein.

Metabolism of 7,9-DMBAC and 7,10-DMBAC by Rat Liver Microsomes. [^{3}H]7,9-DMBAC or [^{3}H]7,10-DMBAC (40 μM, 1 × 10^6 dpm/mL, added in 30 μL of acetone/mL incubation) was incubated at 37 °C with microsomal protein (0.2 mg/mL) in 25 or 13 mL reaction mixtures, respectively, with 0.1 M potassium phosphate buffer (pH 7.4), containing magnesium chloride (3 mM), G-6-P (5 mM), G-6-PDH (1 unit/mL), and NADP (0.5 mM). The mixture was preincubated for 2 min before the metabolism was initiated by the addition of NADP. The incubation mixtures were shaken (70 cycles/min) under air in the dark for 40 min.

At the termination of the reaction, the incubation mixtures were shaken with 2 volumes of ice-cold ethyl acetate to extract metabolites. The aqueous and organic phases were pooled from 15 flasks, the organic phase was separated, and the aqueous phase was reextracted with the same solvent (2 volumes). The combined organic phases were dried with anhydrous Na_2SO_4, and the solvent was removed under reduced pressure at ambient temperatures (<30 °C). The residue was transferred to a Reactivial and redissolved in dimethylformamide (DMF, 2 μL/mL incubation). Material from 20 mL incubations was injected onto the analytical reversed-phase HPLC system to collect the metabolite fractions. Some metabolites were mixtures, demonstrated not to be homogeneous in UV absorption spectra using the peak purity monitor of the Beckman System Gold HPLC software. All metabolites were evaporated to dryness, rechromatographed if necessary on normal-phase silica gel, and purified fractions were trimethylsilylated and subjected to GCMS.

Metabolism of Alcohols Derived from 7,9-DMBAC and 7,10-DMBAC. The metabolism of three hydroxymethyl deriva-

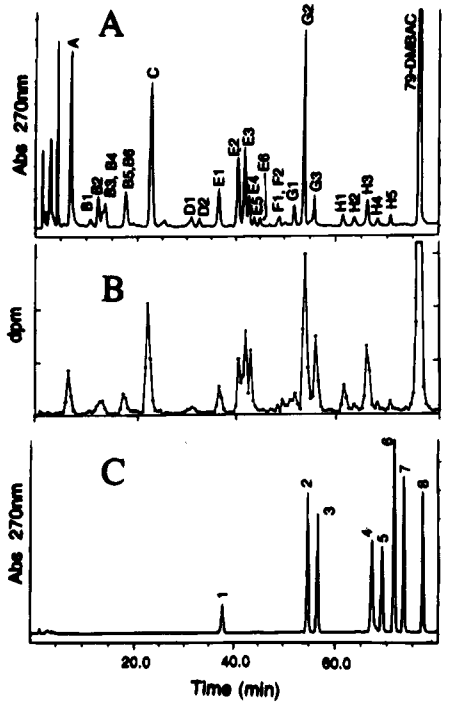

Figure 2. HPLC of 7,9-DMBAC metabolites produced by 3MC-induced liver microsomes. (A) UV absorbance (270 nm), (B) radioactivity, and (C) synthetic standards: **1**, 7,9-diOHMBAC; **2**, 9-OHM-7MBAC; **3**, 7-OHM-9MBAC; **4**, 7,9-DMBAC-5,6-oxide; **5**, 7,9-diacetoxymethyl-BAC; **6**, 9-acetoxymethyl-7MBAC; **7**, 7-acetoxymethyl-9MBAC; **8**, 7,9-DMBAC.

tives of 7,9-DMBAC were studied by incubating synthetic 7-OHM-9MBAC, 9-OHM-7MBAC, and 7,9-diOHMBAC with microsomal protein as described above. The incubations (10 × 1 mL for each) were performed with 0.2 mg/mL microsomal protein at a substrate concentration of 40 μM (added in 30 μL acetone). After 30 min of reaction, the incubation was stopped by addition of ice-cold ethyl acetate (2 mL/1 mL of incubation), and the metabolites and unused substrate were isolated as described for the parent compounds above. Similar incubations were conducted with 7-OHM-10MBAC and 10-OHM-7MBAC at 40 μM substrate for 45 min.

Results

7,9-DMBAC Metabolites. Incubation of 7,9-DMBAC for 40 min with 3MC-induced rat liver microsomal preparations, NADPH, and oxygen (air) produced very extensive metabolism determined to be about 40% of substrate from radiochemical assay of fractions emerging from the reversed-phase HPLC column (Figure 2). More than 24 UV absorbing peaks were seen, and these corresponded to 21 radioactive peaks. Some metabolites cochromatographed with the limited number of available synthetic standards, the alcohols, and 7,9-DMBAC-5,6-oxide. Evidence for the structures of metabolites was derived from cochromatography, the effect of the epoxide hydrolase inhibitor TCPO upon the relative amount of each metabolite produced (Figure 3), and the formation of metabolites from putative primary metabolites, 7-OHM-9MBAC, 9-OHM-7MBAC (Figure 4), and 7,9-diOHMBAC (not shown).

Using the metabolite designations of Figure 2A, product identifications are summarized in Table 1 which shows the HPLC and GC retention times, fragmentation, and structural assignments for each product. Also, chromatographic data obtained with normal-phase chromatography are included. The nature of the products was usually determined by the recognition of the quasi-molecular ions and their characteristic fragmentations.

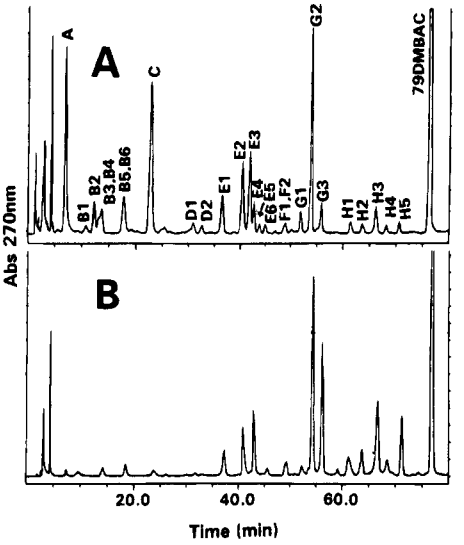

Figure 3. HPLC of 7,9-DMBAC metabolites produced by 3MC-induced liver microsomes in the absence (A) and presence (B) of TCPO.

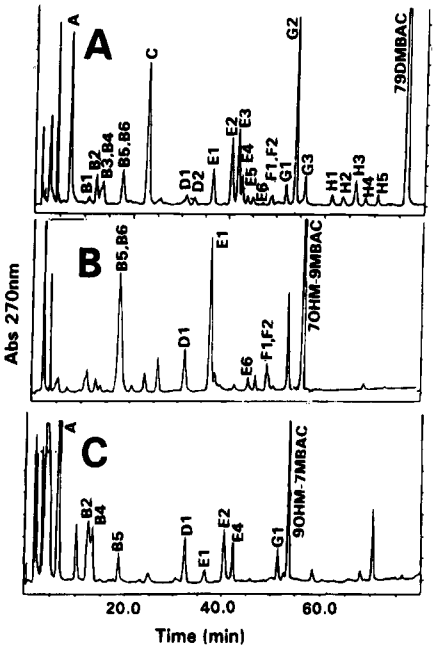

Figure 4. HPLC of 7,9-DMBAC metabolites (A), 7-OHM-9MBAC metabolites (B), and 9-OHM-7MBAC (C) metabolites produced by 3MC-induced liver microsomes.

The ultraviolet absorption spectra were particularly useful in making positional assignments of functional groups by comparison with published spectra obtained for 7MBAC (*23–25*) and benz[*c*]acridine (*26, 27*) derivatives because the reduction at different ring positions affords quite distinct spectra.

7,9-DMBAC Alcohol Metabolites. All possible methyl-oxidized metabolites were formed from 7,9-DMBAC. These were fractions E1, G2, and G3, and they cochromatographed with 7,9-diOHMBAC, 9-OHM-7MBAC, and 7-OHM-9MBAC, respectively (Figure 2A,C). From the UV peak height and from the radiochemical histogram, oxidation at the 9-position was seen to be predominant. When incubations were conducted in which the substrate aza-aromatic hydrocarbon was replaced by each mono(hydroxymethyl) derivative, the bis-alcohol was produced as a major metabolite of 7-OHM-9MBAC but was a minor product of 9-OHM-7MBAC (Figure 4). The HPLC chromatographic behavior of the monoalcohols was distinctive on normal-phase HPLC, the 9-alcohol being more polar.

Table 1. Chromatographic and Mass Spectral Data for 7,9-DMBAC Metabolites

metabolite designation		proposed structure	retention time (min) RP-HPLC[b]	silica HPLC[d]	GC	CIMS data[a] $M + C_3H_5^+$	$M + C_2H_5^+$	MH^+	$MH^+ - 16$	$MH^+ - 90$	other ions
A		9-OHM-7MBAC-5,6-DHD	7.0		6.77	564 (2)	552 (4)	524 (64)	508 (82)	434 (100)	360 (30), 346 (12), 344 (8), 332 (19), 258 (5), 147 (95)
B1		?[e]	10.8		8.13	400 (8)	388 (21)	360 (100)	344 (36)	270 (18)	316 (18)
B2		9-OHM-7MBAC-3,4-DHD	12.3		9.20		552 (6)	524 (36)	508 (80)	434 (100)	346 (46), 332 (25), 258 (40), 191 (70), 147 (58)
B3		?[e]	13.2		10.33	564 (4)	552 (20)	524 (80)	508 (100)	434 (98)	418 (28), 362 (80), 346 (8), 147 (16)
B4		?[e]	13.7		9.95	490 (6)	478 (20)	450 (100)	434 (30)	360 (70)	422 (12), 332 (10), 272 (8), 258 (5)
B5		7,9-diOHMBAC-phenol	17.7		7.33		552 (11)	524 (60)	508 (83)	434 (62)	418 (20), 362 (12), 346 (18), 147 (45)
B6		7-OHM-9MBAC-3,4-DHD	17.7		7.36		552 (5)	524 (22)	508 (100)	434 (90)	360 (19), 346 (43), 344 (15), 332 (28), 258 (22), 191 (92), 147 (82)
C		7,9-DMBAC-5,6-DHD	22.7	13.7	5.28	476 (3)	464 (14)	436 (59)	420 (48)	346 (100)	374 (18), 330 (10), 258 (16), 147 (10)
D1b[c]	a	7,9-diOHMBAC-oxide	31		8.75	474 (2)	462 (11)	434 (45)	418 (20)	344 (46)	328 (20), 258 (48), 147 (100)
	b				9.25	562 (2)	550 (10)	522 (75)	506 (70)	432 (72)	416 (38), 360 (22), 346 (18), 332 (20), 147 (100)
D1a	c	1,2,3,4-tetrahydro-7,9-DMBAC-tetrol			9.41		642 (4)	614 (20)	598 (86)	524 (32)	508 (21), 434 (46), 346 (20), 191 (100), 147 (46)
E1		7,9-diOHMBAC	36.5		8.77	474 (5)	462 (24)	434 (100)	418 (42)	344 (98)	384 (4), 372 (16), 328 (35), 258 (50), 147 (95)
E2		?[e]	40.3		8.71	474 (3)	462 (19)	434 (100)	418 (70)	344 (54)	346 (28), 330 (10), 272 (6), 147 (38)
E3		7,9-DMBAC-3,4-DHD	42		7.80	476 (2)	464 (12)	436 (55)	420 (90)	346 (100)	330 (8), 286 (10), 258 (38), 191 (55), 147 (12)
E4[c]	a	9-OHM-7MBAC-5,6-oxide	43.8		8.27	386 (6)	374 (25)	346 (95)	330 (26)	256 (49)	298 (10), 286 (26), 258 (100), 272 (14), 244 (12)
	b				9.34		462 (10)	434 (56)	418 (22)	344 (30)	362 (8), 330 (8), 274 (12), 147 (100)
E6		?[e]	45.5		9.77	474 (4)	462 (22)	434 (100)	418 (48)	344 (50)	362 (6), 346 (46), 330 (10), 274 (8), 147 (85)
F1[c]	a	7-OHM-9MBAC-5,6-oxide	48.7	13.4[f]	7.00	386 (8)	374 (22)	346 (95)	330 (30)	256 (82)	286 (22), 284 (20), 272 (16), 258 (100), 244 (30)
	b				8.29	474 (2)	462 (15)	434 (82)	418 (40)	344 (50)	274 (24), 272 (15), 258 (10), 147 (100)
F2[c]	a	?[e]	49	11.4	7.98		462 (11)	434 (62)	418 (52)	344 (30)	362 (3), 346 (28), 332 (18), 274 (18), 147 (100)
	b				9.27		462 (22)	434 (100)	418 (38)		362 (10), 346 (15)
G1		?[e]	52	11.0	8.88	400 (5)	388 (20)	360 (100)	344 (20)		332 (10), 316 (3), 288 (3)
G2		9-OHM-7MBAC	54	15.0	8.20	386 (8)	374 (25)	346 (100)	330 (22)	256 (28)	284 (6), 272 (2), 258 (12), 244 (2)
G3		7-OHM-9MBAC	56	10.0	7.00	386 (5)	374 (30)	346 (100)	330 (32)	256 (68)	296 (4), 286 (16), 284 (18), 272 (2), 258 (22), 244 (2)
H1		7,9-DMBAC-phenol	61	6.3	7.99	386 (4)	374 (21)	346 (100)	330 (24)		274 (4)
H2		7,9-DMBAC-phenol	63	9.8	8.18	386 (5)	374 (22)	346 (100)	330 (24)		274 (3)
H3[c]	a	7,9-DMBAC-5,6-oxide	66	7.9	6.29	298 (8)	286 (24)	258 (100)			274 (4)
	b				7.92	386 (3)	374 (15)	346 (100)			274 (4)
H4		?[e]	68		7.16	312 (5)	300 (19)	272 (100)			258 (5), 244 (15)
parent		7,9-DMBAC	76		6.28	298 (6)	286 (30)	258 (100)			

[a] m/z values with relative intensities in parentheses. [b] Gradient elution with aqueous acetonitrile on RP-8 column. [c] Multiple GC peaks are formed during derivatization and GC. [d] Elution with 5% EtOH in hexane fraction unless otherwise stated. [e] No partial structure assigned. [f] A flow rate of 1.5 mL/min was used.

The UV spectra of these 3 alcoholic metabolites were obtained from the diode array detector, and these were identical to those of the synthetic standards. Figure 5 shows the comparison of the spectra of 7-OHM-9MBAC and metabolite G3. Each alcohol displayed a spectrum which closely resembled that of the parent compound and is characteristic of the benz[*c*]acridine chromophore. After derivatization by trimethylsilylation, GC afforded single GC peaks from G2 and G3 which possessed the same retention times as those derived from synthetic standards and fragmented by loss of 16 m/z units (methane) or 90 m/z units (trimethylsilanol) from the

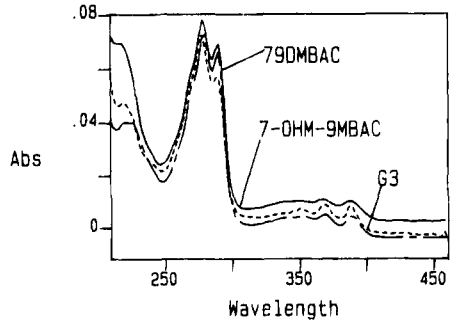

Figure 5. UV spectra of alcohol metabolite G3 of 7,9-DMBAC (- - -), the parent compound (— - —), and authentic synthetic 7-OHM-9MBAC (—).

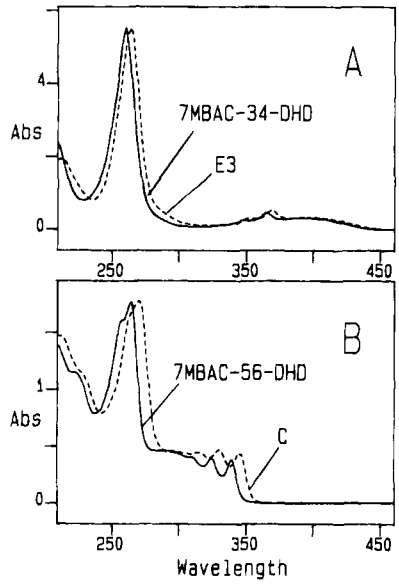

Figure 6. UV spectra of dihydrodiol metabolites of 7,9-DMBAC. (A) Metabolite E3 (- - -) and 7-methylbenz[c]acridine-3,4-DHD (—); (B) metabolite C (- - -) and 7-methylbenz[c]acridine-5,6-DHD (—).

quasimolecular ions at m/z 346. Derivatization and GC of metabolite E1 also afforded a single GC peak with the same retention as that of derivatized 7,9-diOHMBAC. Losses of 16 and 90 m/z from the quasimolecular ion at m/z 434 were major fragmentations. The formation of these metabolite peaks was not affected by the presence of TCPO.

7,9-DMBAC Dihydrodiol Metabolites. The presence of the dihydrodiols was recognized through the effect of TCPO in the incubations which caused almost complete inhibition of formation of metabolite C, and totally eliminated metabolite E3. Neither was formed from the monoalcohols. The UV spectrum of each (Figure 6) was distinctive and very similar in shape to those of 7-methylbenz[c]acridine 3,4-dihydrodiol and 7-methylbenz[c]acridine 5,6-dihydrodiol, respectively, which were available from previous work (*23–25*). These chromophores are characteristic of a 4-vinylacridine (*25–27*) (metabolite E3) rather than of acridine (*28*), and of a 2-phenylquinoline (metabolite C). They were different from the spectra of isomeric DHDs of 7-methylbenz[c]acridine. GC of isolated peaks after derivatization afforded quasimolecular ions at m/z 436 from both C and E3, and these fragmented by loss of 16 or 90 m/z units corresponding to loss of methane or trimethylsilanol, respectively. As well, metabolite E3 showed a strong ion at m/z 191 which is characteristic of bis(trimethylsilyl) derivatives of non-K-region dihydrodiols both in the chemical ionization and electron impact ionization modes (*23, 29–31*). The dihydrodiol nature of metabolite E3, and its UV spectrum which was distinctly different from that of the 3-vinylacridine chromophore in the 1,2-dihydrodiols of benz[c]acridine (*27*) and 7-methylbenz[c]acridine (*25*), allowed the functional group to be placed at the 3,4-position. The mass spectrum of derivatized metabolite C showed no m/z 191 ion, and this taken together with the 2-phenylquinoline UV chromophore allowed the structure 7,9-DMBA-5,6-DHD to be assigned. Sufficient metabolite C was isolated to allow its ^{1}H NMR spectrum to be determined, ppm in MeOH-d_4 (Table 2). The signals due to H_1 (δ 8.51) and H_{11} (δ 7.89) were found significantly upfield from these proton signals in 7,9-DMBAC at 9.50 and 8.21 ppm, respectively. This is consistent with the reduced aromatic system in metabolite C. Two signals at δ 5.34 and 4.86 were assigned to the H_5 and H_6 protons with $J_{5,6}$ = 3.1 Hz, indicating a small dihedral angle (~60°) between these protons, and that the OH groups occupied quasidiaxial positions due to the steric bulk of the 7-methyl and OH group at C_6.

Other Primary Metabolites of 7,9-DMBAC. Other metabolites of this substrate that were not formed by metabolic processing of the 7- or 9-alcohol and which were assigned one functionality only were found in the H-region of the reversed-phase HPLC. H1 and H2 were identified as phenols based on their low polarity (long retention times on reversed-phase HPLC), their formation from 7,9-DMBAC but not from the monoalcohols, and their UV spectra and MS after derivatization. These metabolites emerged from the reversed-phase HPLC as pure compounds judging by the UV heterogeneity monitor. Their UV spectra (Figure 7A) showed little similarity to the parent compound, possessing long wavelength absorptions at about 305 nm in H1 and 402 nm in H2. Spectral and chromatographic standards were not available, but derivatization and GC gave a single chromatographic peak from each with a quasimolecular ion at m/z 346 corresponding to a monotrimethylsilylated derivative. The fragmentation was minimal with peaks being found at MH^+ − methane (m/z 330) and MH^+ − dimethylsilene (72 m/z lower at 274). No loss of trimethylsilanol occurred. The metabolite peaks were therefore assigned as phenols, but the position of their OH functional group was unknown. When synthetic 7,9-DMBAC-5,6-oxide was derivatized, two GC peaks were obtained, only one of which was due to a phenolic derivative (see below). This peak, which must bear the hydroxyl group at the 5- or 6-position, was distinct from those obtained from H1 and H2, making it unlikely that H1 or H2 is functionalized in the K-region.

Metabolite peak H3 was homogeneous by UV, and its proportion of total metabolites increased in the presence of TCPO. It cochromatographed with authentic 7,9-DMBAC-5,6-oxide and possessed an identical UV spectrum (Figure 7B) which was virtually the same as that of metabolite peak C apart from a bathochromic shift of about 3 nm for H3. Trimethylsilylation and GCMS afforded two chromatographic peaks, the first of which (~10% of total) was identical in spectrum and retention time with that obtained from 7,9-DMBAC. The second was a trimethylsilylated derivative of a phenol. The appearance of such peaks is similar to the behavior of K-region arene oxides of other polycyclic aromatic compounds (*23, 30, 32, 33*) although benzo[a]pyrene 4,5-oxide was not reported to undergo deoxygenation (*31*). The second peak possessed a quasimolecular ion and a mass spectrum virtually identical to those from derivatized H1 and H2. These data allowed the unequivocal assignment

Table 2. ^{1}H NMR Spectra of 7,9-DMBAC and Metabolite C

compound	chemical shift[a] (ppm) and coupling constant (Hz)							
	H_1	H_2–H_4	H_5	H_6	H_8	H_{10}	H_{11}	other
7,9-DMBAC[b]	9.50	7.60–7.80	7.60 (d)	7.90 (d)	7.89	7.58 (d)	8.21 (d)	2.93 (7-Me); 2.56 (9-Me)
$J_{5,6}$ = 9.5; $J_{10,11}$ = 8.5 Hz								
metabolite C[c]	8.51	7.47 - 7.55	5.34 (d)[d]	4.86 (d)[d]	7.94	7.58 (dd)	7.99 (d)	2.82 (7-Me); 2.56 (9-Me)
$J_{5,6}$ = 3.1; $J_{10,11}$ = 8.6; $J_{8,10}$ = 1.80 Hz								

[a] Multiplicities: doublet (d) or doublet of doublets (dd). [b] $CDCl_3$. [c] Methanol-d_4. [d] These assignments may be reversed.

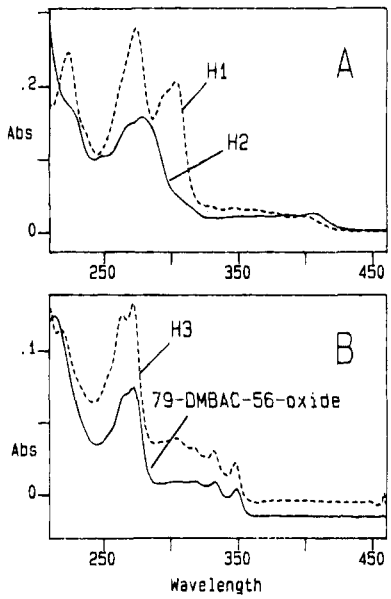

Figure 7. UV spectra of 7,9-DMBAC metabolites. (A) H1 (- - -) and H2 (—); (B) H3 (- - -) and 7,9-MBAC-5,6-oxide (—).

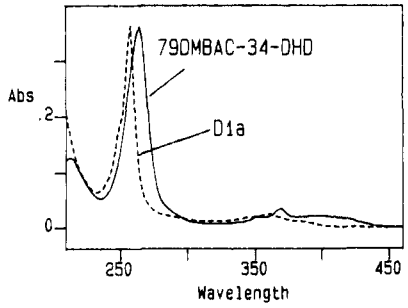

Figure 8. UV spectra of 7,9-DMBAC metabolites D1a (- - -) and E3, 7,9-DMBAC-3,4-DHD (—).

of the structure of H3 as 7,9-DMBAC-5,6-oxide. When the oxide was chromatographed on a reversed-phase HPLC column with unbuffered aqueous methanol, decomposition to other peaks was observed with the 5,6-dihydrobenz[*c*]acridine UV chromophore.

Secondary Metabolites of 7,9-DMBAC. These include 7,9-diOHMBAC described above. They are formed from 9-OHM-7MBAC (metabolite peaks A, B2, B4, E2, E4, and G1), from 7-OHM-9MBAC (peaks B6, E6, F1, and F2), or from either (B5 and D1) (Figure 4). Only metabolite D1b was formed from the alcohols, D1a being formed through another pathway. Partial structural conclusions were based on the formation of each set of metabolites from one or the other monoalcohol.

Only one secondary product not derived through an alcohol was detected. Peak D1 was resolved by further reversed-phase HPLC with a slower gradient into separate peaks D1a and D1b. TCPO completely inhibited formation of metabolite D1a, and its UV spectrum (Figure 8) was that of the parent acridine (*28*) with λ_{max} at 248 nm, some 14–15 nm lower than that of metabolite E3, 7,9-DMBAC-3,4-dihydrodiol. Trimethylsilylation of

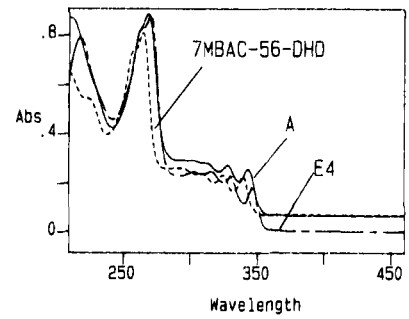

Figure 9. UV spectra of 7,9-DMBAC metabolites A (—), E4 (— - —) and 7MBAC-5,6-DHD (- - -).

the mixture, D1, and GC afforded 3 peaks, one of which possessed a quasimolecular ion at *m*/*z* 614 corresponding to a fully derivatized tetrahydrotetraol. Ions at *m*/*z* 524 and 434 indicated two sequential losses of trimethylsilanol. As well, an ion at *m*/*z* 191 (base peak) showed that a vicinal dihydrodiol function was present at a non-K-region. The UV spectrum and the mass fragmentation of the *m*/*z* 614 peak allowed the structure 7,9-DMBAC-1,2,3,4-tetrahydrotetraol to be tentatively assigned.

Metabolite D1b was tentatively ascribed as an arene oxide of 7,9-diOHMBAC. Derivatization and GC afforded two chromatographic peaks. The first possessed the same retention time as derivatized 7,9-diOHMBAC and had the same quasimolecular ion at *m*/*z* 434 while the second peak had MH^+ at 522 corresponding to a tris-trimethylsilylated phenol. This lost 90 *m*/*z* units from MH^+ to form *m*/*z* 432 and afforded a significant ion at *m*/*z* 360, 72 *m*/*z* units lower than the ion at 432. These two GC peaks were consistent with an arene oxide function which can lose oxygen thermally in the GC or during derivatization (*23, 30, 32*).

Metabolites A and E4 were formed from 9-OHMBAC and possessed UV spectra (Figure 9) characteristic of species with a reduced K-region, comparable with that of metabolite C (also shown). The formation of A was decreased when incubations were conducted in the presence of TCPO. Derivatization and GC afforded a single peak for A, with a quasimolecular ion at *m*/*z* 524, and two GC peaks for E4, where the early eluting one corresponded to the derivative of 9-OHMBAC and the latter to a bis-trimethylsilylated derivative of a phenolic alcohol (MH^+ at *m*/*z* 434 and loss of dimethylsilene or 72 *m*/*z* units). Structures proposed for metabolite A and E4 are 9-OHM-7MBAC-5,6-DHD and 9-OHM-7MBAC-5,6-oxide, respectively. Metabolite peak B2 was also a dihydrodiol derived from 9-OHM-7MBAC. Its formation was prevented when epoxide hydrolase was inhibited by TCPO, and its UV spectrum (maxima at 263*,[3] 348, and 367 nm) was very similar to those of metabolites D1a and E3 with the characteristic 4-vinylacridine moiety (*25–27*). Derivatization and GCMS afforded a single tris-trimethylsilylated peak, and therefore, B2 was assigned

[3] In UV spectra given in the text, the most intense peak is indicated with an asterisk.

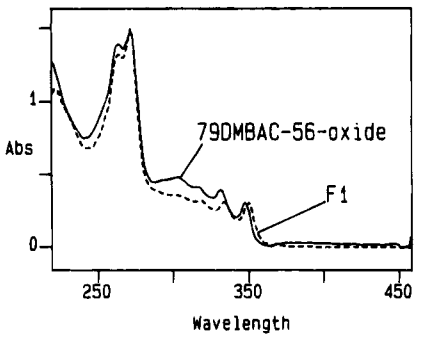

Figure 10. UV spectra of 7,9-DMBAC metabolites F1 (- - -) and H3, 7,9-DMBAC-5,6-oxide (—).

as 9-OHM-7MBAC-3,4-DHD with 3,4-dihydrobenz[*c*]acridine chromophore. By similar arguments peak B6 which possessed the UV spectrum (λ_{max} 262*, 350, and 369 nm) of a 4-vinylacridine and was obtained from 7-OHM-9MBAC and 7,9-DMBAC, but not from 9-OHM-7MBAC, was assigned as 7-OHM-9MBAC-3,4-DHD.

Reversed-phase metabolite peak F was recognized to be a mixture by use of the diode array detector and was separated into two peaks, F1 and F2, on normal-phase HPLC. Fraction F1 possessed a UV spectrum characteristic of a 5,6-dihydrobenz[*c*]acridine (Figure 10) and afforded two GC peaks after derivatization, the earlier eluting one being the derivative of 7-OHM-9MBAC, while the second was a derivative of a phenolic alcohol. The GC was typical of the K-region oxide function (*23, 30, 32, 33*), and F1 was therefore assigned as 7-OHM-9MBAC-5,6-oxide.

7,10-DMBAC Metabolites. From the isomeric dimethylbenz[*c*]acridine ([^{3}H]7,10-DMBAC) several metabolites were formed in rat liver microsomes from 3MC-pretreated male rats. Conversion to products more polar than unchanged substrate was high with incubation times greater than 20 min (34–61% for 20–60 min). The metabolic products were separated from one another and unchanged substrate by reversed-phase HPLC using an acetonitrile–water gradient affording more than 19 ultraviolet absorbing peaks, and radioactivity was found in 17 of these (Figure 11). Through the use of the two monofunctional alcohols as substrate (Figure 12) and methods described for 7,9-DMBAC, 17 metabolite peaks were identified as metabolites of the parent compounds and 5 were recognized to be metabolic products of these alcohols (Table 3).

7,10-DMBAC Alcohol Metabolites. Metabolite peaks H1, H2, and E cochromatographed with 10-OHM-7MBAC, 7-OHM-10MBAC, and 7,10-di-OHMBAC, respectively (Figure 11A,C). The UV spectra of the three metabolites were very similar to each other and that of the parent compound 7,10-DMBAC. A comparison of the UV spectra of metabolite H1 and authentic 10-OHM-7MBAC is shown (Figure 13). After derivatization by trimethylsilylation the metabolites possessed retention times identical with those of the derivatized reference alcohols, and the CIMS showed, besides the methane adduct ions, mass fragmentation evidence that they were benzylic trimethylsilyl ethers by loss of methane or trimethylsilanol. The relative amounts of these three metabolites were usually increased when incubations were conducted in the presence of the epoxide hydrolase inhibitor TCPO (Figure 14). The 10-alcohol was the predominant alcohol, and when these monoalcohols were used as substrates, the 10-OHM-7MBAC gave less oxidation to the bis-alcohol derivative. These metabolite peaks

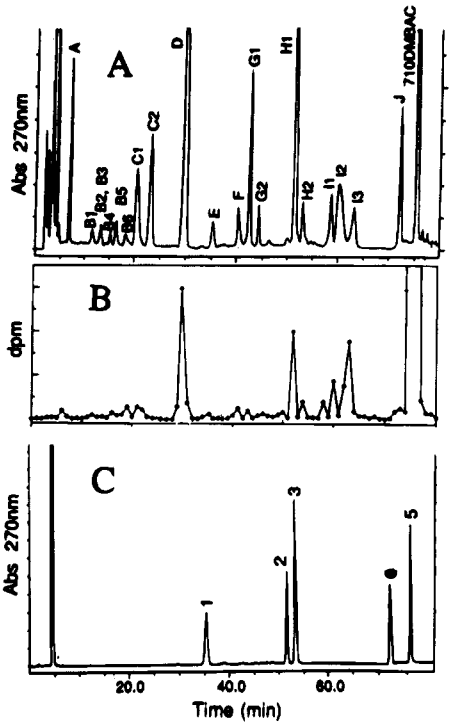

Figure 11. HPLC of 7,10-DMBAC metabolites produced by 3MC-induced rat liver microsomes. (A) UV absorption (270 nm), (B) radioactivity, and (C) synthetic standards: **1**, 7,10-diOHMBAC; **2**, 10-OHM-7MBAC; **3**, 7-OHM-10MBAC; **4**, 10-acetoxymethyl-7MBAC; **5**, 7,10-DMBAC.

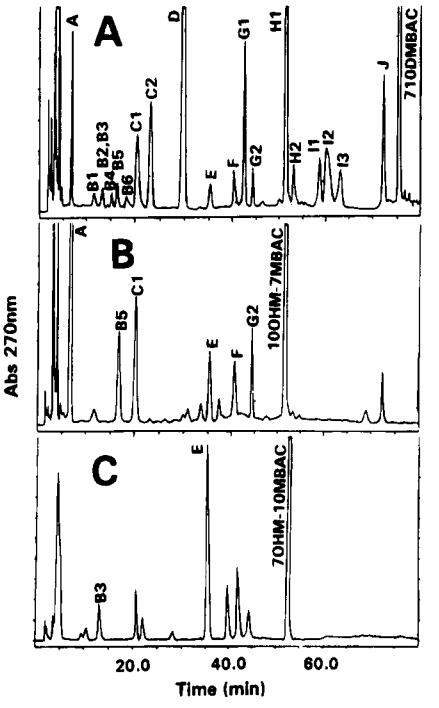

Figure 12. HPLC of metabolites of 7,10-DMBAC (A), 10-OHM-7MBAC (B), and 7-OHM-10MBAC (C) produced by 3MC rat liver microsomes.

were assigned structures 10-OHM-7MBAC, 7-OHM-10MBAC, and 7,10-di-OHMBAC, respectively, for H1, H2 and E.

7,10-DMBAC Dihydrodiols. Monofunctionalized dihydrodiol oxidation products were found as metabolites only of the parent hydrocarbon and not from either of the monoalcohols. Their formation was either reduced or prevented when incubations were conducted in the presence of TCPO (Figure 14).

Table 3. Chromatographic and Mass Spectral Data for 7,10-DMBAC Metabolites

metabolite designation		proposed structure	retention time (min) RP-HPLC[b]	silica HPLC[d]	GC	CIMS data[a] M + $C_3H_5^+$	M + $C_2H_5^+$	MH^+	$MH^+ - 16$	$MH^+ - 90$	other ions
A		10-OHM-7MBAC-5,6-DHD	6.8		6.33	564 (3)	552 (8)	524 (30)	508 (54)	434 (72)	418 (3), 360 (18), 346 (10), 332 (8), 272 (12), 258 (4), 147 (100)
B1		?[f]	11.8		7.68	564 (4)	552 (18)	524 (75)	508 (62)	434 (100)	462 (16), 418 (18), 346 (3), 274 (3), 147 (30)
B2		?[f]	13.1		7.33	564 (4)	552 (20)	524 (82)	508 (95)	434 (100)	474 (4), 462 (18), 452 (2), 418 (31), 346 (8), 274 (2), 147 (20)
B3		?[f]	13.1		9.04	564 (4)	552 (25)	524 (100)	508 (55)	434 (88)	462 (12), 418 (20), 390 (48), 346 (12), 191 (16), 147 (18)
B4		?[f]	15.4		8.62	564 (3)	552 (23)	524 (100)	508 (68)	434 (80)	462 (12), 452 (2), 418 (22), 390 (42), 346 (8), 191 (14), 147 (15)
B5		10-OHM-7MBAC-3,4-DHD	16.9		10.96	564 (2)	552 (6)	524 (38)	508 (100)	434 (90)	474 (2), 462 (12), 418 (12), 360 (8), 346 (25),191) 147 (22)
B6		?[f]	18.0		8.44	564 (3)	552 (20)	524 (95)	508 (40)	434 (100)	462 (14), 452 (3), 418 (18), 390 (42), 346 (15), 274 (6), 191 (15), 147 (35)
C1		10-OHM-7MBAC-8,9-DHD	20.3		7.28	564 (2)	552 (8)	524 (32)	508 (5)	434 (14)	418 (21), 344 (58), 272 (22), 258 (8), 191 (21), 147 (100)
C2		7,10-DMBAC-5,6-DHD	23.1		5.07	476 (3)	464 (14)	436 (56)	420 (43)	346 (100)	386 (2), 374 (15), 330 (10), 286 (4), 272 (12), 258 (15), 147 (8)
D		7,10-DMBAC-8,9-DHD	29.9		6.46	476 (4)	464 (21)	436 (87)	420 (20)	346 (100)	374 (12), 330 (10), 302 (60), 258 (12), 191 (22), 147 (11)
E		7,10-diOHMBAC	35.6		7.94	474 (3)	462 (18)	434 (82)	418 (42)	344 (85)	384 (4), 372 (13), 328 (28), 272 (15), 258 (22), 244 (26), 147 (100)
F[c]	a	10-OHM-7MBAC-5,6-oxide	41.4		7.41	386 (3)	374 (15)	346 (100)	330 (34)	256 (75)	286 (8), 284 (4), 272 (6), 258 (50), 244 (6)
	b				8.61	474 (3)	462 (12)	434 (76)	418 (42)	344 (48)	272 (12), 147 (100)
G1		7,10-DMBAC-3,4-DHD	43.0		7.88	476 (3)	464 (11)	436 (55)	420 (92)	346 (100)	386 (2), 374 (10), 330 (8), 286 (6), 258 (34), 191 (42), 147 (10)
G2		10-OHM-7MBAC-phenol	45.2		9.98	474 (4)	462 (21)	434 (100)	418 (72)	344 (32)	362 (2), 330 (5), 147 (12)
H1		10-OHM-7MBAC	51.8		7.44	386 (5)	374 (21)	346 (100)	330 (40)	256 (84)	286 (10), 284 (5), 272 (6), 258 (45), 244 (4)
H2		7-OHM-10MBAC	53.5		6.47	386 (2)	374 (23)	346 (100)	330 (35)	256 (90)	286 (12), 284 (20), 272 (6), 258 (52), 244 (22)
I1		7,10-DMBAC-phenol	59.0	9.2[e]	8.38	386 (4)	374 (22)	346 (100)	330 (36)		274 (2)
12a		7,10-DMBAC-phenol	60.0	9.4	8.68	386 (5)	374 (23)	346 (100)	330 (20)		274 (9)
I2b		5- or 6-hydroxy-7,10-DMBAC	60.0	11.0	8.27	386 (3)	374 (25)	346 (100)	330 (22)		274 (5)
I2c		9- or 8-hydroxy-7,10-DMBAC	60.0	12.6	8.56	386 (3)	374 (21)	346 (100)	330 (12)		274 (3)
I3a[c]	a	7,10-DMBAC-5,6-oxide	63.0	6.9	6.73	298 (6)	286 (28)	258 (100)			
	b				8.24	386 (3)	374 (18)	346 (100)	330 (15)		274 (4)
I3b[c]	a	7,10-DMBAC-8,9-oxide	63.0	5.5	6.75	298 (4)	286 (22)	258 (100)			
	b				8.50	386 (3)	374 (16)	346 (100)	330 (16)		274 (6)
parent		7,10-DMBAC	75.6		6.72	298 (5)	286 (24)	258 (100)			

[a] m/z values with relative intensities in parentheses. [b] Gradient elution with aqueous acetonitrile on RP-8 column. [c] Multiple GC peaks are formed during derivatization and/or GC process. [d] Elution with 10% EtOAc in hexane fraction unless otherwise noted. [e] Elution with 3% EtOH in hexane fraction at 1.0 mL/min. [f] No partial structure assigned.

Metabolite G1 possessed a 4-vinylacridine chromophore which is obtainable by reduction of the benzo ring, and its UV spectrum was very similar to that of 7MBAC-3,4-DHD (*25*) apart from a small bathochromic shift of 2–3 nm (Figure 15A). Trimethylsilylation afforded a derivative which on GC gave only one chromatographic peak with a quasimolecular ion at m/z 436 and expected methane adducts at m/z 464 and 476. Loss of trimethylsilanol from MH^+ afforded the base ion at m/z 346, and the spectrum included a pronounced ion at m/z 191 typical of trimethylsilyl derivatives of non-K-region dihydrodiols. This, and the UV spectral data, allowed the

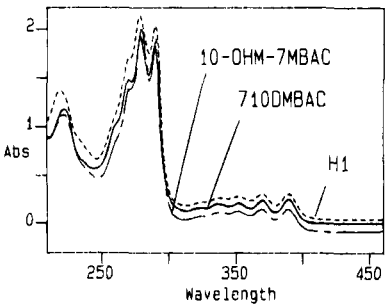

Figure 13. UV spectra of alcohol metabolite H1 of 7,10-DMBAC (- - -), the parent compound (—), and authentic synthetic 10-OHM-7MBAC (— - —).

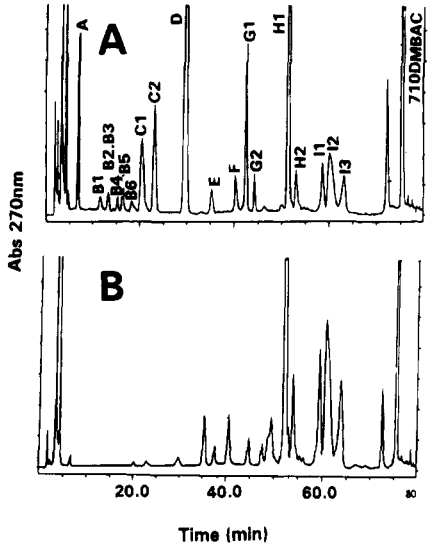

Figure 14. HPLC of 7,10-DMBAC metabolites formed in the absence (A) and presence (B) of TCPO.

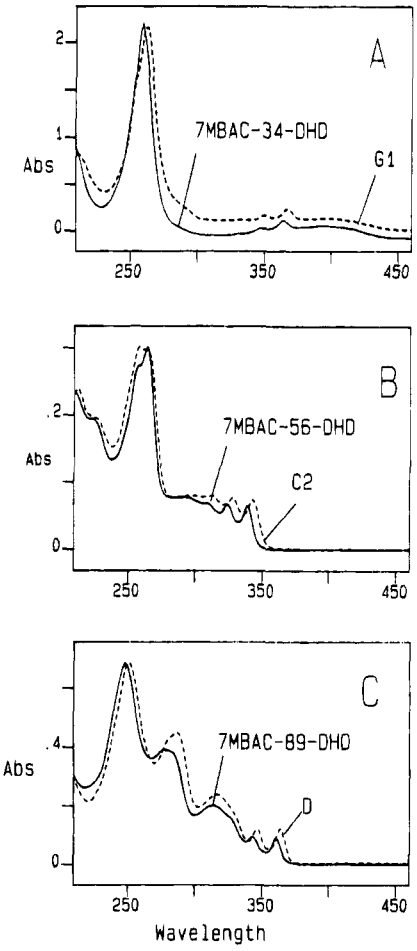

Figure 15. UV spectra of dihydrodiol metabolites of 7,10-DMBAC. (A) G1 (- - -) and 7-methylbenz[*c*]acridine-3,4-DHD (—); (B) C2 (- - -) and 7-methylbenz[*c*]acridine-5,6-DHD (—); (C) D (- - -) and 7-methylbenz[*c*]acridine-8,9-dihydrodiol (—).

structure of the metabolite to be assigned as 7,10-DMBAC-3,4-DHD.

Metabolite D was the major dihydrodiol and a major metabolite formed in incubations with 3MC-induced rat liver microsomes. Its UV spectrum (Figure 15C) was almost identical to that of 7MBAC-8,9-DHD apart from a small bathochromic shift that would be expected for the extra methyl group, and it was distinct from those of isomeric 7MBAC dihydrodiols (*25, 27*). GCMS after trimethylsilylation gave a single chromatographic peak with MH^+ at m/z 436. Loss of trimethylsilanol to give m/z 346 and the presence of a pronounced ion at m/z 191 were taken as evidence that the functional group was not at the K-region. Sufficient material was isolated to allow its ^1H NMR spectrum to be obtained (Table 4), and this allowed confirmation of the structural assignment as a 7,10-DMBAC-8,9-DHD. The absence of one aromatic methyl signal, and its replacement by a singlet at 2.19 ppm (allylic), indicated that the 8,9,10,11-ring was no longer fully aromatic and that functionalization occurred in that ring. The two methine protons at C_8 and C_9 gave signals for the dihydrodiol function and were weakly coupled ($J_{8,9}$ = 2.1 Hz), showing that the conformation of this functional group is affected by the nearby methyl groups. The dihedral angle between the two CH groups was near 60°, and the hydroxyl groups were quasidiaxial. The assignments followed comparisons with the parent compound, and decoupling and NOE experiments.

The third dihydrodiol was assigned as 7,10-DMBAC-5,6-DHD based on its UV spectrum (Figure 15B) which was characteristic of the reduced K-region, and GCMS after derivatization. The ions observed in the single GC peak were those seen with the other dihydrodiols with the exception that the ion at m/z 191 was not present in the derivative of C2. The latter was significant for metabolites G1 and D. This supports the assignment of the functional group at the 5,6-position, the K-region.

The order of elution from reversed-phase HPLC of these three metabolites was consistent with patterns observed for dihydrodiols of 7MBAC (*23, 33*), benzanthracene (*34*), methylbenzanthracenes (*35*), and 7,9-DMBAC. In all cases the 5,6-dihydrodiol is most polar and emerges first, and the 3,4-dihydrodiol is least polar.

Other Primary Metabolites of 7,10-DMBAC. These metabolites, bearing a single functional group, were phenols (I1, I2a, I2b, and I2c) and arene oxides (I3a and I3b). Relative amounts of the latter were increased when TCPO inhibited epoxide hydrolase in the incubations (Figure 14).

Metabolite I1 was homogeneous by the UV spectral monitor and also gave a single peak on normal-phase HPLC. Its UV spectrum (Figure 16A) was distinct from that of the parent compound. Fraction I2 was a mixture which was separated on normal-phase chromatography into 3 peaks (I2a, I2b, I2c) with characteristic UV spectra and different retention times on GC after derivatization. Each of these metabolites was phenolic and gave a single GC peak with MH^+ at m/z 346 but no substantial fragmentation apart from the loss of 16 m/z units from the quasimolecular ion occurred. The UV spectrum of I2b was very similar to that of 5-OH-7MBAC, and after derivatization and GC we obtained a peak with the same

Table 4. ^{1}H NMR Spectra of 7,10-DMBAC and Two Metabolites

compound	chemical shift[a] (ppm) and coupling constants (Hz)							
	H_1	H_2–H_3 H_4 or H_2–H_4	H_5	H_6	H_8	H_9	H_{11}	other
7,10-DMBAC[b]	9.52	7.75–7.85	7.72 (d)	8.04 (d)	8.16 (d)	7.45 (dd)	8.15	3.09 (7-Me); 2.64 (10-Me)
$J_{5,6}$ = 9.3; $J_{8,11}$ = 0.5; $J_{9,11}$ = 1.7 Hz								
metabolite D[c]	9.33	7.69–7.76	8.0 7.90 (d)	8.08 (d)	5.23 (d)	4.25 (d)	6.75 (q)	2.86 (7-Me); 2.19 (10-Me, d)
$J_{2,4}$ = 3.2; $J_{3,4}$ = 6.2; $J_{5,6}$ = 9.4; $J_{8,9}$ = 2.1; $J_{10Me,11}$ = 1.5 Hz								
10-OHM-7MBAC[b]	9.53	7.67–7.88	na[d]	8.04 (d)	8.27 (d)	7.56	8.32	3.08 (7-Me); 4.99 (10-CH_2)
$J_{5,6}$ = 9.0; $J_{8,9}$ = 9.0 Hz								
metabolite C1[c]	9.34	7.70–7.78	8.0 7.91 (d)	8.09 (d)	5.26 (d)	4.36 (d)	7.00 (t)	2.86 (7-Me); 4.43, 4.55 (10$H_a$$H_b$, 2 dd)
$J_{5,6}$ = 9.1; $J_{8,9}$ = 2.2; $J_{10\text{-methylene},11}$ = 1.7; $J_{10Ha,10Hb}$ = 15.5 Hz								

[a] Multiplicities are shown as doublet (d), triplet (t), quartet (q), doublet of doublets (dd). [b] $CDCl_3$. [c] Acetone-d_6. [d] Not assigned.

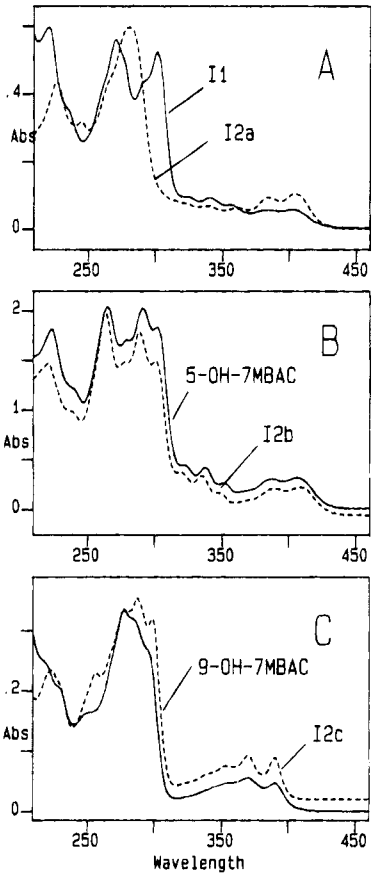

Figure 16. UV spectra of 7,10-DMBAC metabolites in the I region. (A) I1 (—) and I2a (- - -); (B) I2b (- - -) and 5-hydroxy-7-methylbenz[*c*]acridine (—); (C) I2c (- - -) and 9-hydroxy-7-methylbenz[*c*]acridine (—).

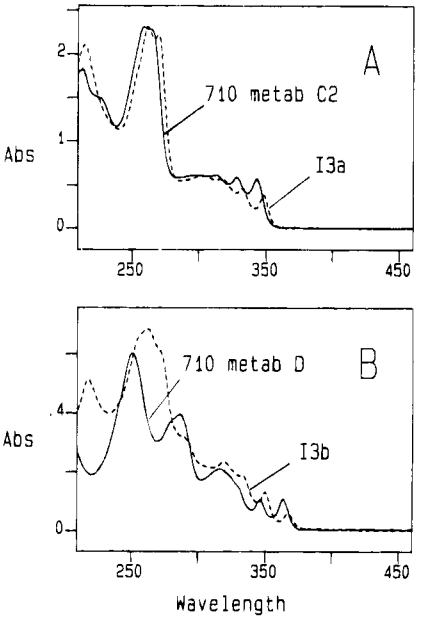

Figure 17. UV spectra of 7,10-DMBAC arene oxide metabolites. (A) I3a (- - -) and C2, 7,10-DMBAC-5,6-DHD (—); (B) I3b (- - -) and D, 7,10-DMBAC-8,9-DHD (—).

retention time as the major peak derived from metabolite I3a, the 5,6-oxide. Therefore, fraction I2b was assigned the structure 5- or 6-OH-7,10-DMBAC. Metabolite fraction I2c was tentatively assigned as the 8- or 9-phenol on the basis of its UV spectrum which was similar to that of 9-OH-7MBAC and its chromatographic behavior after derivatization. The single peak chromatographed at the same retention as the major product from reaction of 8,9-oxide (see below) under silylation conditions, and the derivatized acid-catalyzed dehydration product from 7,-10-DMBAC-8,9-DHD.

Metabolite fraction I3 separated into 2 pure compounds on normal-phase chromatography. The less polar, I3a, displayed a UV spectrum closely related to those of 7,9-DMBAC-5,6-oxide and metabolite C2, identified as 7,10-DMBAC-5,6-dihydrodiol. The UV spectrum of the second showed some similarities to metabolite D, 7,10-DMBAC-8,9-dihydrodiol (Figure 17). Trimethylsilylation of each and GCMS afforded 2 peaks. The earlier eluting minor peak corresponded to 7,10-DMBAC and was formed by deoxygenation of arene oxides under silylation conditions or, if there is underivatized material, in the injection port (*23, 30, 32, 33*). The second peaks were monotrimethylsilyloxy derivatives of 7,10-DMBAC (MH^+ *m/z* 364), which underwent little mass spectral fragmentation. On the basis of the UV chromophores of these I3 metabolites, their reaction under silylation conditions, and their formation when epoxide hydrolase was inhibited, I3a and I3b were assigned as the 5,6-oxide and 8,9-oxide, respectively.

Secondary Metabolites of 7,10-DMBAC. These were derived from 10-OHM-7MBAC, 7-OHM-10MBAC, or other primary metabolites. Metabolites A, B5, C1, F, and G2 were formed from the 10-alcohol, metabolite B3 was formed from the 7-alcohol, and the other 4 metabolites found in the B region of the HPLC were formed from other primary metabolites.

Metabolites A, B5, and C were assigned as dihydrodiols of 10-OHM-7MBAC based on their formation from the alcohol and their much reduced abundance when incubations of the parent compound were conducted in the presence of TCPO (Figure 14). Peak A was a minor product of 7,10-DMBAC but a major product from the 10-alcohol. Its UV spectrum (Figure 18A) was characteristic of the system with the reduced K-region and was very similar to that of the 5,6-dihydrodiol (peak C2) and 7MBAC-5,6-DHD. Trimethylsilylation and chromatography afforded one GC peak with MH^+ at *m/z* 524, and prominent loss of trimethylsilanol and methane occurred

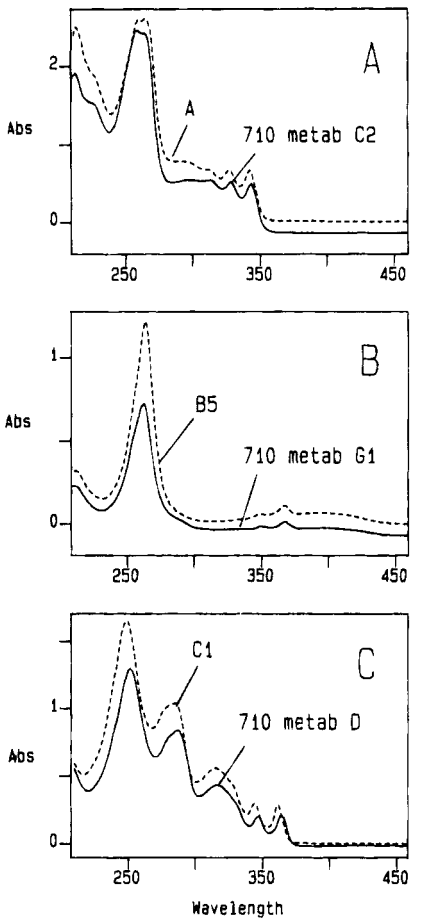

Figure 18. Dihydrodiol metabolites of 10-OHM-7MBAC and 7-OHM-10MBAC. (A) A (- - -) and C2, 7,10-DMBAC-5,6-DHD (—); (B) B5 (- - -) and G1, 7,10-DMBAC-3,4-DHD (—); (C) C1 (- - -) and D, 7,10-DMBAC-8,9-DHD (—).

to afford ions at m/z 434 and 508, respectively. The absence of an ion at m/z 191 was consistent with the placement of the functional group at the K-region (*23, 29–31*), and this metabolite was assigned as 10-OHM-7MBAC-5,6-DHD. Fraction B5 possessed the 4-vinylacridine UV chromophore (Figure 18B), and its spectrum was virtually identical to those of 7,10-DMBAC-3,4-DHD (G1) and 7,9-DMBAC-3,4-DHD (see Figure 6). The single peak found after derivatization and GC was typical of a tris-trimethylsilyl derivative of a dihydrodiol alcohol with the quasimolecular ion at m/z 524 and associated fragmentation. The presence of a prominent m/z 191 ion indicated that the dihydrodiol function was not at the K-region, and the structure 10-OHM-7MBAC-3,4-DHD was assigned. Metabolite peak C1 possessed a distinctive UV spectrum of the 8,9-reduced aromatic system found in the 8,9-dihydrodiol (Figure 18C). This similarity of UV absorption spectra to those of 7,10-DMBAC-8,9-DHD and 7MBAC-8,9-DHD (Figure 18C), and the CIMS of the single peak obtained in the GC after derivatization, allowed the structure 10-OHM-7MBAC-8,9-DHD to be assigned. The mass spectrum displayed ions from the loss of trimethylsilanol (90 m/z units) and a significant ion at m/z 191 as found in the spectra of other non-K-region trimethylsilylated dihydrodiol derivatives (*23, 29–31*). The placement of the functional group at the 8,9-position was confirmed from the ^{1}H NMR spectrum (Table 4). Comparison with the spectra of metabolite D and 10-OHM-7MBAC indicated that the 8,9,10,11-ring was altered. Compared with the alcohol, the signals from H_9 and H_{11} were upfield, while they were downfield from the equivalent signals found in the spectrum of D. The

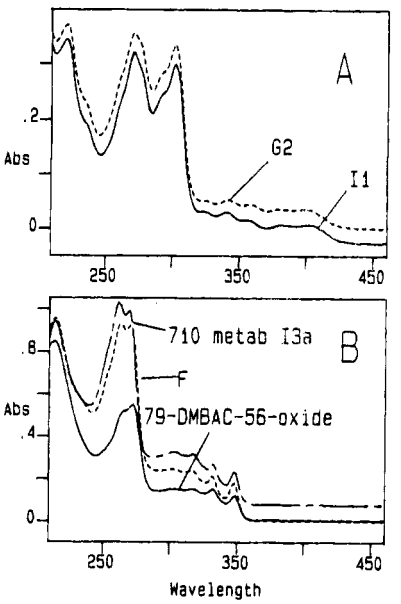

Figure 19. Secondary metabolites not derived from 10-OHM-7MBAC. (A) G2 (- - -) and I1, a phenol (—); (B) F (- - -), I3a, 7,-10-DMBAC-5,6-oxide (— - —), and 7,9-DMBAC-5,6-oxide (—).

10-methylene protons were no longer chemically equivalent and displayed strong geminal coupling. This probably occurs via the formation of an intramolecular H-bond between the 9- and 10-hydroxyl groups. The presence of the 7-methyl signal at a slightly shielded position due to the 8,9-dihydrodiol function is consistent with the structural assignment.

Metabolites F and G2 were formed when epoxide hydrolase was inhibited, indicating that they were not dihydrodiols. A phenolic structure for G2 was suggested by the identity of its UV spectrum with that of 7,10-DMBAC phenol I1 (Figure 19A), and this assignment was supported by the mass spectrum after derivatization when a bis-trimethylsilylated derivative was obtained with MH^+ at m/z 434. Loss of methane (16 m/z units) or trimethylsilanol (90 units) but not dimethylsilene (72 units) were predominant fragmentation pathways. Metabolite F possessed the UV spectrum of a K-region reduced entity (Figure 19B) and after derivatization and GC afforded two chromatographic peaks. The first, formed by thermal deoxygenation (*23, 30, 32, 33*), emerged with the same retention as the derivative of 10-OHM-7MBAC and possessed the same CIMS. The second, which possessed an MH^+ at m/z 434 and corresponded to a bis-trimethylsilylated species, would be obtained from an arene oxide of 10-OHM-7MBAC. The structure 10-OHM-7MBAC-5,6-oxide was tentatively assigned for F.

Only one secondary metabolite, B3, was derived from 7-OHM-10MBAC during incubations of the parent compound with liver microsomes. This is in accord with the low relative amount of the 7-alcohol compared with that of the 10-alcohol. Metabolite peak B3 (λ_{max} 252*, 291, 329, 355, and 373 nm) was separated from metabolite B2 using a more gradual gradient elution on the reversed-phase column and, after GCMS of the derivatized material, afforded a single peak. The quasimolecular ion at m/z 524 corresponding to a tris-trimethylsilyl derivative, and the presence of an ion at m/z 191 was consistent with the presence of a dihydrodiol function at a position other than the 5,6. However, no position for the dihydrodiol function was assigned because the UV spectrum did not show close correspondence to other UV data. The

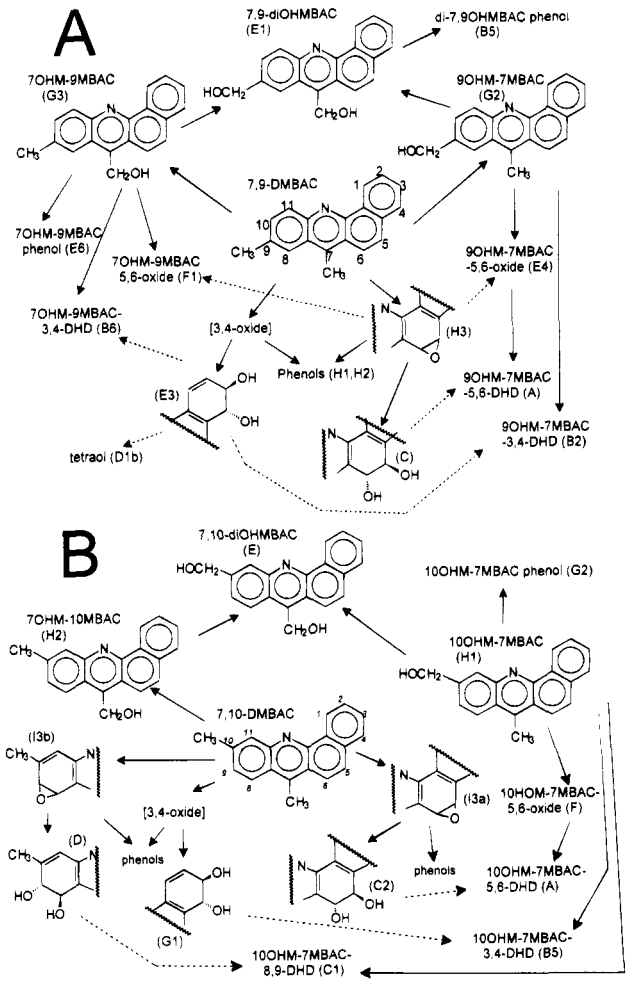

Figure 20. Scheme showing pathway of 3MC-induced rat liver microsomal metabolism of 7,9-DMBAC (A) and 7,10-DMBAC (B).

secondary metabolites, B1, B2, B4, and B6, were not formed from the alcohols. These metabolites were homogeneous and afforded GC peaks corresponding to tris-trimethylsilylated derivatives. This is consistent with phenolic dihydrodiols, but no further characterization was made.

Three HPLC peaks, D2 and H5 from 7,9-DMBAC and J from 7,10-DMBAC, were artifacts. These were formed by ester exchange with the solvent, ethyl acetate, used during isolation of the metabolites. These were 9-(acetoxymethyl)-7MBAC-3,4-dihydrodiol (D2), 9-(acetoxymethyl)-7MBAC (H5), and 10-acetoxy-7MBAC (J), and their structures were proved from their UV and mass spectra, and for H5 and J only, cochromatography with authentic materials.

Discussion

More than 15 metabolites were fully or partially characterized from each of 7,9-DMBAC and 7,10-DMBAC. These pathways are shown in Figure 20. These aza-aromatic polycyclic carcinogens are structurally analogous to several monomethyl benz[*a*]anthracenes and 7,12-dimethylbenz[*a*]anthracene (7,12-DMBA) which are carcinogenic and have been investigated to define their bioactivation pathways (*6, 7*).

The predominant oxidation at the sp^3 hybridized benzylic carbon over oxidation of aromatic carbon seen in compounds such as 7,12-DMBA (*6*) was also seen in the metabolism of 7,9-DMBAC when only 5 of 16 characterized liver microsomal products bore 2 intact methyl groups. For the 7,10-isomer, 9 of 17 metabolites were shown to possess 2 unaltered methyl groups. In the radiochemical histograms of 7,9-DMBAC metabolites, the only products with intact methyl groups which were quantitatively substantial were C and H3. Hydroxylation at the sp^3 hybridized carbon occurs more readily on the methyl on the terminal 8,9,10,11-ring than at the 7-methyl (Figure 2A,B and Figure 11A,B). The 7-hydroxy compounds, H2 from 7,10-DMBAC and G3 from 7,9-DMBAC, were relatively minor products. This was supported by the ease of formation of the bis-alcohols, E1 and E, respectively, from each monoalcohol of 7,9-DMBAC and 7,10-DMBAC (Figures 4 and 12). Investigations of the formation and metabolism of alcohol derivatives of the methyl polycyclic aromatic hydrocarbons have been reported (*7, 36, 37*). Extensive oxidation of methyl groups was seen in the rat liver microsomal metabolism of 6-methylquinoline and 8-methylquinoline (*2*). 3MC-induced preparations afforded about 65% of the (hydroxymethyl)quinolines as the major metabolites. For 7,12-DMBA (*36*), alcohols constituted about 26% of total metabolites formed by 3MC-induced rat liver microsomes, while 7-OHM12MBA afforded about 20% of the dialcohol.

7,12-DMBA (*6, 34, 36*), benz[*a*]anthracene (*34, 38, 39*), and 7-methylbenz[*a*]anthracene (*35*) afforded dihydrodiols on incubation with rat liver microsomes at the 3,4-, 5,6-, 8,9-, and 10,11-positions, and from 7,12-DMBA four dihydrodiol alcohols were characterized which were derivable from each alcoholic oxidation product of the parent (*6*). With the benzacridines in the present study the methyl group blocked formation of the 8,9-dihydrodiol in 7,9-DMBAC and the 10,11-dihydrodiol in 7,10-DMBAC. The former gave the 3,4- and 5,6-dihydrodiols while the latter gave the 3,4-, 5,6-, and 8,9-dihydrodiols. The absence of dihydrodiols with methyl groups attached directly to the dihydrodiol function is in contrast to results obtained with 4-methylbenz[*a*]anthracene and its 6-methyl, 8-methyl, and 10-methyl isomers (*7, 40*). In each case a dihydrodiol was formed at the methyl-substituted position, these being the methylbenz[*a*]anthracene 3,4-, 5,6-, 8,9-, and 10,11-dihydrodiols, respectively. Dihydrodiol metabolites formed at methylated double bonds are generally minor products compared with other dihydrodiols. Similarly, 7-methylbenzo[*a*]pyrene afforded the 7,8-dihydrodiol as a minor metabolite in polychlorinated biphenyl induced rat liver microsomes (*37*). Such a pathway was not found for 5-methylchrysene studies in which neither the 5,6- nor the 11,12-positions was oxidized (*41*). The UV spectra of the various dihydro derivatives of benz[*c*]acridine are characteristic and distinctly different from each other (*23*). Were any 79-DMBAC-8,9-dihydrodiol or 7,10-DMBAC-10,11-dihydrodiol formed, these must be formed as minor products. Metabolites were not assigned with functional groups at the 1,2-positions. This position is almost refractory to oxidation in the polycyclic and aza-aromatic hydrocarbons.

The isolation of a stable K-region oxide without the inhibition of the liver microsomal epoxide hydrolase with compounds such as TCPO has previously been observed for 7-methylbenz[*c*]acridine (*23*), dibenz[*a,j*]acridine (*30*), dibenz[*c,h*]acridine (*42*), and dibenz[*a,h*]acridine (*43*). Only in the presence of TCPO did benzo[*h*]quinoline afford the 5,6-epoxy-5,6-dihydroquinoline, the K-region dihydrodiol normally being produced (*44*). Both 7,9-DMBAC and 7,10-DMBAC formed K-region oxides in the absence of enzyme inhibition, and there were small

increases in their relative amounts formed in the presence of TCPO (for H3, 20–26% with 7,9-DMBAC; and for I3, 24–38% with 7,10-DMBAC). Somewhat surprising was the detection of metabolites tentatively identified as 7,10-DMBAC-8,9-oxide. Evidence for this rests on UV spectra and behavior on derivatization for GC. Another example of this type of metabolite is the formation of 6-methylquinoline 7,8-oxide from 6-methylquinoline (*2*). Generally, metabolism of homocyclic PAH systems has led to no oxides as isolable compounds without interference with the epoxide hydrolase.

The metabolic formation of dihydrodiols with *trans* stereochemistry from arene oxides occurs by the *trans* addition of water (*45–47*). This configuration is generally proven by comparison with synthetic standards in which the configuration has been determined by the synthesis and confirmed by the ^{1}H NMR coupling constants of the methine protons (*23, 30*). In these dihydrodiols, the hydroxyl groups are usually quasidiequatorial, being intramolecularly hydrogen bonded, and the dihedral angle between the methine protons is usually about 150°. In the present work the dihydrodiols were not synthesized, and because the coupling constants for the methine protons were available and small (2–3 Hz) for 7,9-DMBAC-5,6-dihydrodiol (Table 2) and 7,10-DMBAC-8,9-dihydrodiol and its 10-OHM-derivative (Table 4), the stereochemistry could not be determined. This follows because there is a peri interaction between one methyl group, that at the 7-position, and one hydroxyl group (at the 6- or 8-position) which forces the diol into the quasidiaxial conformation. Therefore, the ^{1}H NMR data did not reveal the stereochemistry of the products. From the evidence available from the literature on the formation of dihydrodiols in mammalian system (*3, 10, 48*), the stereochemistry of these products was assigned as *trans*.

Several products from each methylated benz[*c*]acridine studied in this work were functionalized with a dihydrodiol at the 3,4-position. These were B2, B6, and E3 from 7,9-DMBAC and B5 and G1 from 7,10-DMBAC. Each of these derivatives has a "bay-region" double bond which may be further oxidized to afford a "bay-region" diol epoxide. Such compounds have been implicated in the bioactivation of polycyclic aromatic hydrocarbons and their isosteric aza analogues (*10, 48*). For example, 7MBAC-3,4-dihydrodiol is the only tumorigenic dihydrodiol obtained from 7MBAC, and it is more potent than the parent compound (*4*). In mutagenicity studies it was highly active toward *Salmonella typhimurium* (strain TA100) with metabolic activation, while the derivative *anti*-7MBAC-3,4-diol-1,2-epoxide was active toward Chinese hamster V79 cells in the absence of metabolic activation (*29*). The *syn* isomer of this diol epoxide was only weakly active by comparison. One stereoisomer of the 3,4-diol 1,2-epoxides of dibenz[*c,h*]acridine (1*R*,2*S*,3*S*,4*R*) possessed six times the tumorigenicity of the parent compound and other diol epoxides (*10*). The bay-region diol epoxides of dibenz[*a,j*]acridine were mutagenic in the Ames test and toward V79 cells without metabolic activation (*49*). The 3,4-dihydrodiols of 6-methylbenz[*a*]anthracene and its 7- and 8-methyl isomers, 7,12-dimethylbenz[*a*]anthracene, 12-(hydroxymethyl)-7-methylbenz[*a*]anthracene, and 7-(hydroxymethyl)benz-[*a*]anthracene were all, at least, equally potent as mutagens or carcinogens as their parent hydrocarbons (*12*). The metabolic products of 7,9-DMBAC and 7,10-DMBAC which possess the 3,4-dihydrodiol function are highly mutagenic in the Ames test[4] and may be expected to be more carcinogenic than their metabolic precursors, the fully aromatic compounds. The stereochemistry of dihydrodiol formation is important in the bioactivation of polycyclic aromatic compounds. The *R,R*-isomers of the dihydrodiol are generally more active than their enantiomers (*10, 48*). The stereochemistry of the monofunctionalized dihydrodiols formed in the present study has also been investigated, and the *R,R*-enantiomers predominate.[5] The results of the present study showing the formation of 3,4-dihydrodiols, the optical composition of these, and their mutagenicity[4,5] suggest that 7,9-DMBAC and 7,10-DMBAC are bioactivated by pathways similar to those found for other PAH and PAAH.

Acknowledgment. This work was financially supported by the National Health and Medical Research Council of Australia, and by the Department of Employment, Education and Training through the award of an Overseas Postgraduate Research Scholarship to Y.Y. The assistance of Bruce Tattam and Helen Elimelakh is also gratefully acknowledged.

References

(1) LaVoie, E. J., Adams, E. A., Shigematsu, A., and Hoffmann, D. (1983) On the metabolism of quinoline and isoquinoline: possible molecular basis for differences in biological activities. *Carcinogenesis* **4**, 1169–1173.

(2) Scharping, C. E., Duke, C. C., Holder, G. M., and Larden, D. (1993) The hepatic metabolism of two methylquinolines. *Carcinogenesis* **14**, 1041–1047.

(3) Warshawsky, D. (1992) Environmental sources, carcinogenicity, mutagenicity, metabolism, and DNA binding of nitrogen and sulfur heterocyclic aromatics. *Environ. Carcinog Rev.* **C10**, 1–71.

(4) Chang, R. L., Levin, W., Wood, A. W., Shirai, N., Ryan, A. J., Duke, C. C., Jerina, D. M., and Holder, G. M. (1986) High tumorigenicity of the 3,4-dihydrodiol of 7-methylbenz[c]acridine on mouse skin and in the newborn mouse. *Cancer Res.* **46**, 4552–4555.

(5) Lacassagne, A., Buu-Hoi, N. P., Daudel, R., and Zajdela, F. (1956) The relation between carcinogenic activity and the physical properties of angular benzacridines. *Adv. Cancer Res.* **4**, 315–369.

(6) Chou, M. W., and Yang, S. K. (1979) Combined reversed-phase and normal-phase high performance liquid chromatography in the purification and identification of 7,12-dimethylbenz[a]anthracene metabolites. *J. Chromatogr.* **185**, 635–654.

(7) Yang, S. K. (1988) Metabolism and activation of benz[a]anthracene and methylbenz[a]anthracenes. In *Polycyclic aromatic hydrocarbon carcinogenesis: structure activity relationships* (Yang, S. K., and Silverman, B. D., Eds.) Vol. 1, pp 129–150, CRC Press, Boca Raton, FL.

(8) Sawicki, E., Meeker, J. E., and Morgan, M. J. (1965) The qualitative composition of air pollution source effluents in terms of aza-heterocyclic compounds and polynuclear aromatic hydrocarbons. *Int. J. Water Pollut.* **9**, 291–298.

(9) Epstein, S. S. (1967) Carcinogenicity of organic extracts of atmospheric pollutants. *J. Air Pollut. Control Assoc.* **17**, 728–729.

(10) Lehr, R. E., Wood, A. W., Levin, W., Conney, A. H., and Jerina, D. M. (1988) Benzacridines and dibenzacridines: metabolism, mutagenicity carcingenicity. In *Polycyclic aromatic hydrocarbon carcinogenesis: structure activity relationships* (Yang S. K., and Silverman, B. D., Eds.) Vol. I, pp 31–58, CRC Press, Boca Raton.

(11) Sugiyanto, Scharping, C. E., McManus, M. E., Birkett, D. J., Holder, G. M., and Ryan, A. J. (1992) The formation of proximate carcinogens from three polycyclic aromatic compounds by human liver microsomes. *Xenobiotica* **11**, 1299–1307.

(12) Wislocki, P. G., and Lu, A. Y. H. (1988) Carcinogenicity and mutagenicity of proximate and ultimate carcinogens of polycylic aromatic hydrocarbons. In *Polycyclic aromatic hydrocarbon carcinogenesis: structure activity relationships* (Yang S. K., and Silverman, B. D., Eds.) Vol. I, pp 1–30, CRC Press, Boca Raton.

(13) Glatt, H., Seidel, A., Ribeiro, O., Kirkby, C., Hirom, P., and Oesch, F. (1987) Metabolic activation to a mutagen of 3-hydroxy-*trans*-

[4] Y. Ye, C. E. Scharping, and G. M. Holder, unpublished results.
[5] Y. Ye, C. C. Duke, and G. M. Holder, unpublished results.

7,8-dihydroxy-7,8-dihydrobenzo[a]pyrene, a secondary metabolite of benzo[a]pyrene. *Carcinogenesis* **8**, 1621–1627.
(14) Buu-Hoi, N. P., and Lecocq, L. (1944) Chemistry of inhibitors of carcinogenic hydrocarbons: synthesis of polymethylbenzacridines. *C. R. Hebd. Seances Acad. Sci.* **218**, 792–794.
(15) Pene, C., Lhoste, J. M., Markovits, P., and Hubert-Habart, M. (1976) Synthesis of 7,10- and 7,8-dimethylbenz[c]acridine. *J. Chem. Soc., Perkin Trans. I*, 2277–2279.
(16) Ye, Y., Holder, G. M., and Duke, C. C. (1993) The preparation of ^{2}H- and ^{3}H-labelled 7,9-, and 7,10-dimethylbenz[c]acridine by catalytic dehalogenation. *J. Labelled Compd. Radiopharm.* **33**, 1–10.
(17) Ravi, B. N., and Wells, R. J. (1982) A series of new diterpenes from the brown alga, *Dilophus marginata* (Dictyotaceae). *Aust. J. Chem.* **35**, 129–144.
(18) Buu-Hoi, N. P. (1951) The chemistry of carcinogenic nitrogen compounds. II. Further derivatives of 1:2- and 3:4-benzacridine. *J. Chem. Soc.*, 670–695.
(19) Knoevenagel, E. (1914) Catalytic efficacy of iodine. *J. Prakt. Chem.* **89**, 171–183.
(20) Krishan, S., Kuhn., D. G., and Hamilton, G. A. (1977) Direct oxidation in high yield of some polycyclic aromatic compounds to arene oxides using hypochlorite and phase transfer catalysts. *J. Am. Chem. Soc.* **99**, 8121–8123.
(21) Lowry, O. H, Rosebrough, N. J., Farr, A. L., and Randall, R. J. (1951) Protein measurement with Folin phenol reagent. *J. Biol. Chem.* **193**, 265–275.
(22) Omura, T., and Sato, R. (1972) The carbon monoxide binding pigment of liver microsomes. II. Solubilization, purification and properties. *J. Biol. Chem.* **239**, 2370–2385.
(23) Boux, L. J., Duke, C. C., Holder, G. M., Ireland, C. M., and Ryan, A. J. (1983) Metabolism of 7-methylbenz[c]acridine: comparison of rat liver and lung microsomal preparations and the identification of some minor metabolites. *Carcinogenesis* **4**, 1429–1435.
(24) Ireland, C. M., Cheung, H. T. A., Holder, G. M., and Ryan, A. J. (1982) Rat liver microsomal metabolites of 7-methylbenz[c]-acridine. *Chem.-Biol. Interact.* **40**, 305–318.
(25) Duke, C. C., Murphy, P. M., and Holder, G. M. (1984) Synthesis of the non-K-region dihydrodiols of the carcinogen, 7-methylbenz-[c]acridine. *J. Org. Chem.* **49**, 4446–4451.
(26) Schaefer-Ridder, M., and Engelhardt, U. (1981) Synthesis of *trans*-3,4-dihydroxy-3,4-dihydrobenz[a]- and -[c]acridines, possible proximate carcinogenic metabolites of polycyclic azaarenes. *J. Org. Chem.* **46**, 2895–2899.
(27) Lehr, R. E., and Kumar, S. (1981) Synthesis of dihydrodiol and other derivatives of benz[c]acridine. *J. Org. Chem.* **46**, 3675–3681.
(28) Stern, E. S., and Timmons, C. J. (1970) *Gillam and Stern's Introduction to electronic absorption spectroscopy in organic chemistry*, 3rd Ed., pp 169–171, Edward Arnold, London.
(29) Wong, L. K., Wang, C.-L. A., and Daniel, F. B. (1979) Mass spectral characterization of the K-region and non K-region dihydrodiols of 7,12-dimethylbenz[a]anthracene. *Biomed. Mass Spectrom.* **6**, 305–308.
(30) Gill, J. H., Duke, C. C., Rosario, C. A., Holder G. M., and Ryan, A. J. (1986) Dibenz[a,j]acridine metabolism: identification of metabolites formed in vitro by liver microsomes from 3-methylcholanthrene induced rats. *Carcinogenesis* **7**, 1371–1378.
(31) Takahashi, G., Kinoshita, K., Hashimoto, K., and Yasuhira, K. (1979) Identification of benzo[a]pyrene metabolites by gas chromatograph–mass spectrometer. *Cancer Res.* **39**, 1814–1818.
(32) Patel, J. R., Griffin, G. W., and Laseter, J. L. (1978) Determination of arene oxides by a gas chromatography mass spectrometry system: thermal reactions of 9,10-epoxy-9,10-dihydrophenanthrene. *Anal. Lett.* **B11**, 239–247.
(33) Gill, J. H., Bonin, A. M., Podobna, E., Baker, R. S. U., Duke, C. C., Rosario, C. A., Ryan A. J., and Holder, G. M. (1986) 7-Methylbenz[c]acridine: mutagenicity of some of its metabolites and derivatives, and the identification of trans-3,4-dihydro-3,4-dihydroxy-7-methylbenz[c]acridine as a microsomal metabolite. *Carcinogenesis* **7**, 23–31.
(34) Tierney, B., Hewer, A., MacNicholl, A. D., Gervasi, P. G., Rattle, H., Walsh, C., Grover, P. L., and Sims, P (1978) The formation of dihydrodiols by the chemical and enzymatic oxidation of benz[a]-anthracene and 7,12-dimethylbenz[a]anthracene. *Chem.-Biol. Interact.* **23**, 243–257.
(35) Tierney, B., Hewer, A., Walsh, C., Grover, P. L., and Sims, P. (1977) The metabolic activation of 7-methylbenz[a]anthracene in mouse skin. *Chem.-Biol. Interact.* **18**, 179–193.
(36) Chou, M. W., Yang, S. K., Sydor, W., and Yang, C. S. (1981) Metabolism of 7,12-dimethylbenz[a]anthracene and 7-hydroxymethyl-12-methylbenz[a]anthracene by rat liver nuclei and microsomes. *Cancer Res.* **41**, 1559–1564.
(37) Wong, T. K., Chiu, P. L., Fu, P. P., and Yang, S. K. (1981) Metabolic study of 7-methylbenz[a]pyrene with rat liver microsomes: separation by reversed-phase and normal-phase high performance liquid chromatography and characterization of metabolites. *Chem.-Biol. Interact.* **36**, 153–166.
(38) Thakker, D. R., Levin, W., Yagi, H., Turujman, S., Kapadia, D., Conney, A. H., and Jerina, D. M. (1979) The absolute stereochemistry of the trans dihydrodiols formed from benz[a]anthracene by liver microsomes. *Chem-Biol. Interact.* **27**, 145–161.
(39) Thakker, D. R., Levin, W., Yagi, H., Ryan, D., Thomas, P. E., Karle, J. M., Lehr, R. E., Jerina, D. M., and Conney, A. H. (1978) Metabolism of benz[a]anthracene to its tumorigenic 3,4-dihydrodiol. *Mol. Pharmacol.* **15**, 138–153.
(40) Mushtaq, M., Fu, P. P. F., Miller, D. W., and Yang, S. K. (1985) Metabolism of 6-methylbenz[a]anthracene by rat liver microsomes and mutagenicity of metabolites. *Cancer Res.* **45**, 4006–4014.
(41) Hecht, S. S., Melikian, A. A., and Amin, S. (1988) Effect of methyl substitution on the tumorigenicity and metabolic activation of polycyclic aromatic hydrocarbons. In *Polycyclic aromatic hydrocarbon carcinogenesis: structure activity relationships* (Yang S. K., and Silverman, B. D., Eds.) Vol. 1, pp 95–128, CRC Press, Boca Raton, FL.
(42) Thakker, D. R., Shirai, N., Levin, W., Ryan, D. E., Thomas, P. E., Lehr, R. E., Conney, A. H., and Jerina, D. M. (1985) Metabolism of dibenz[a,h]acridine by rat liver microsomes and by cytochrome P450c with and without added epoxide hydrolase. *Proc. Am. Assoc. Cancer Res.* **26**, 114.
(43) Steward, A. R., Kumar, S., and Sikka, H. C. (1987) Metabolism of dibenz[a,h]acridine by rat liver microsomes. *Carcinogenesis* **8**, 1043–1050.
(44) LaVoie, E. J., Adams, E. A., and Hoffmann, D. (1983) Identification of metabolites of benzo[f]quinoline and benzo[h]quinoline formed by a rat liver homogenate. *Carcinogenesis* **4**, 1133–1138.
(45) Jerina, D. M., and Daly, J. W. (1974) Arene oxides: a new aspect of drug metabolism. *Science* **185**, 572–582.
(46) Sims, P., and Grover, P. L. (1974) Epoxides in polycyclic aromatic hydrocarbon metabolism and carcinogenesis. *Adv. Cancer Res.* **20**, 165–274.
(47) Oesch, F. (1980) Microsomal epoxide hydrolase. In *Enzymatic basis of detoxication* (Jackoby, W. B., Ed.) Vol. II, pp 277–290, Academic Press, New York.
(48) Thakker, D. R., Yagi, H., Levin, W., Wood, A. W., Conney, A. H., and Jerina, D. M. (1985) Polycyclic aromatic hydrocarbons: metabolic activation to ultimate carcinogens. In *Bioactivation of Foreign Compounds* (Anders, M. W., Ed.) pp 177–242, Academic Press, Orlando.
(49) Bonin, A. M., Rosario, C. A., Duke, C. C., Baker, R. S. U., Ryan, A. J., and Holder, G. M. (1989) The mutagenicity of dibenz[a,j]-acridine, some metabolites and other derivatives in bacteria and mammalian cells. *Carcinogenesis* **10**, 1079–1084.

TX940075E